

Municipal Solid waste (MSW) Diversion from  
Landfills: Recycling and Waste to Energy facilities

# Abstract

Municipal solid waste is one of the leading problems of modern world. In the current scenario most of the solid waste is diverted towards the landfill. Disposing MSW in landfills cannot be considered a safe and sustainable solution. Thus there is an immediate need to divert MSW from landfills and process it in a better and more sustainable manner. This thesis explores the difficulties experienced in completely diverting MSW to recycling facilities and achieving total recovery of resources. Many proponents who favor diverting MSW from landfills focus on only increased recycling as the solution. This establishes a premise that it is possible to achieve zero waste to landfills through increased recycling efforts. Complete material recovery from paper and plastic waste streams has been a pivotal point for the success or failure of achieving zero waste targets. The highest reported recovery of material from paper and plastic waste streams are 85% and 73% respectively. Although the recovery of paper from waste in Lombardia, Italy, and of plastics from waste in Lee and Orange Counties, Florida, was nearly 80%, equivalent recovery has not been achieved in other streams. However, the question that arises is what happens to the remaining 15% and 27% of paper and plastic waste and what limitations exist to impede their recovery? Due to technical limitation of the current equipment used for recycling, it is not possible to completely recycle all papers and plastic. For example, state-of-the-art recycling equipment used for paper still has a 66.4% recovery rate (50,000 tons) from 2008-2013 although the amount of paper available for recycle is near 78,000 tons. Plastic recycling is a similar case where a maximum of only 79% can be technically recovered due to problems associated with tensile and impact strength requirements. Importantly, these limitations are independent of the actual market available for the recycled material. These limitations make it necessary to try alternative methods to divert MSW from landfills. One such approach is diverting residual MSW to Waste to energy plants (WtEs). However, the residual ash produced from such facilities are considered unusable waste due to its tendency to leach heavy metals into the environment. Understanding the ash and its composition can help in limiting leaching of heavy metals. Behavior of ash depends on various factors: temperature of furnace, type of compound that leaching elements are present in, presence of calcium-aluminum-silicates (CAS) and matrix composition of the particle. Vitrified CAS matrix can improve the leaching characteristics of ash drastically. For example, lead can be present in as  $\text{PbO}$  or  $\text{PbO}_2$ , the latter being more stable under an acidic environment. This too adds to leaching performance of ash. Also, identifying a marker element or property of ash which can help in identifying leaching characteristics can help in better management of ash. Silicon and Aluminum can be used as a marker to identify the performance of ash under acid attacks. Presence of silicon in ash in the range of 6-20 wt.% mostly indicates towards an ash with low leachability. Understanding these behaviors can help in tuning WTE operations to produce ash with low leaching. Thus, leading towards a sustainable solutions for diverting the MSW towards WtEs. In summary, due to technical performance limitations not all material can be recycled even

if collected as pure streams. The residual that arises from either poor separation or from recycling equipment limitations can be managed in ways other than landfill. The preferred method is to extract energy from those residuals via WTE facilities. The ash that is produced from the WTE operations need to have beneficial uses. If some of the leaching issues are mitigated WTE ash will find more widespread use. The combination of increased recycling, energy recovery from the residuals and widespread use of the ash is the only path toward a zero waste to landfill future.

# Contents

<b>Contents</b>	<b>3</b>
<b>List of Tables</b>	<b>5</b>
<b>List of Figures</b>	<b>6</b>
<b>I RECYCLING</b>	<b>7</b>
<b>1 Introduction</b>	<b>8</b>
1.1 Zero Waste . . . . .	8
<b>2 Recycling</b>	<b>11</b>
2.1 Paper Waste . . . . .	11
2.1.1 Limitations in Paper recycling . . . . .	11
2.2 Plastic Waste . . . . .	16
2.2.1 Limitations in Plastic recycling . . . . .	16
2.3 Metal Waste . . . . .	22
2.3.1 Limitations in Metal recycling . . . . .	22
2.4 Glass Waste . . . . .	23
2.4.1 Limitations in Glass recycling . . . . .	23
2.5 Residual Waste . . . . .	25
<b>II WASTE TO ENERGY FACILITIES</b>	<b>27</b>
<b>3 Waste to Energy Facilities</b>	<b>28</b>
3.1 Overview . . . . .	28
3.2 Experimental Methodology/Techniques . . . . .	29
3.2.1 Sample preparation . . . . .	29
3.2.2 X-Ray powder diffraction spectroscopy (XRPD) . . . . .	30
3.2.3 SEM/EDS . . . . .	32
3.2.4 Inductively coupled plasma atomic emission spectroscopy . . . . .	34
<b>4 Results and Discussion</b>	<b>36</b>
4.1 Matrix of the ash particle . . . . .	36
4.2 Variation in compounds . . . . .	40
4.3 Leaching and behavior under acid attack . . . . .	42
4.4 Summary . . . . .	45

<i>CONTENTS</i>	4
<b>References</b>	48

# List of Tables

2.1	Communities achieving high rates of recycling selected on the basis of amount waste recycled. [5] [4]	12
2.2	Tensile and Tear Index of Pulp as a function of recycle iteration	12
2.3	Effect of enzyme on freeness, tensile and tear index [3]	13
2.4	Breaking length as a function of recycle iteration (Sulphite pulp)[6]	13
2.5	Waste Characterization data for different types of paper waste (2014) [9]	15
2.6	Recovery Estimates for Paper in Processing Facilities (2014) [9]	15
2.7	Communities selected on the basis of amount waste recycled (Plastic) [5] [4]	17
2.8	Experimental values for polymer separation from waste stream by NIR sensors [11]	18
2.9	Waste Characterization data for plastics (2014)	20
2.10	Recovery Estimates for Plastic in Processing Facilities (2014) [9]	21
2.11	Glass specification for recycling	24
3.1	Ash particles classified based on their sizes and hardness	29
4.1	SEM / EDS Measurement of Composition (% w/w)	39
4.2	Compound type of lead from XRD DATA (Regulatory threshold is 5ppm)	41
4.3	ICP-OES Concentrations in Leachate, HNO <sub>3</sub> acid attack	42
4.4	Lead Leached (Calculated)	45
4.5	Summary	47

# List of Figures

1.1	Zero Waste Concept . . . . .	8
1.2	Composition of the municipal solid waste stream . . . . .	9
1.3	Current waste processing strategies in USA. ( Source: EPA annual report 2012) . . . . .	10
2.1	Effect of enzyme in grams per tonne of pulp (TP) on tensile strength . .	14
2.2	Effect of PE contamination in PP stream on (a) Elasticity and (b) Impact properties. [6] . . . . .	18
2.3	Effect of Impact modifier on recycled blend plastic (ORBP - Optimal Recycle Blend Plastic, VPC - Virgin Polycarbonate, IM - Impact modifier) [13] . . . . .	19
2.4	Extract of the Ellingham diagram for some oxides [7] [8] . . . . .	23
2.5	The optimum recovery achieved by different communities for different waste streams. . . . .	25
3.1	Bragg's Law . . . . .	30
3.2	XRD profiles of sample with standard scans of matched compounds . . .	31
3.3	Matched compounds list from figure 3.2 with reference numbers and quantifications . . . . .	31
3.4	SEM schematic . . . . .	32
3.5	Example SEM image using Back Scatter Detector (BSD) . . . . .	33
3.6	EDS schematic . . . . .	34
4.1	Comparison of large (GL) and small particles (GS) form source G . . . .	37
4.2	Comparison of large (DL) and small particles (DS) form source D . . . .	37
4.3	Iron and coppber deposit on large ash particle surface . . . . .	38
4.4	Comparison of different types of depositions on ash particle surface . . .	38
4.5	Cluster of Iron rich particles trapped in a vitrified ash majorly made of Aluminum, Silicon and Calcium. (a) SEM image of a vitrified matrix; b), c) and d) show iron (red), aluminim(blue), silicon (yellow)and calcium (green) . . . . .	40
4.6	Comparison of XRD of Ash from source F & G for Lead compounds . . .	41
4.7	Silicon vs Lead/ Aluminum (ppm) . . . . .	43
4.8	Silicon vs Lead leached . . . . .	43
4.9	Silicon vs Aluminum released (during the acid attack) . . . . .	44

Part I

**RECYCLING**



# Chapter 1

## Introduction

This part of the Thesis presents an understanding to the problems associated in achieving zero waste just through recycling, reuse and reducing waste. An attempt has been made to understand if the concept of achieving Zero waste without landfill and waste-to energy systems are technically feasible or not. This is an introductory chapter and we will discuss what a Zero waste concept is. Why is it important and what is the generally accepted methodology of achieving it. It is essential to understand the philosophy behind the zero waste concept.

### 1.1 Zero Waste

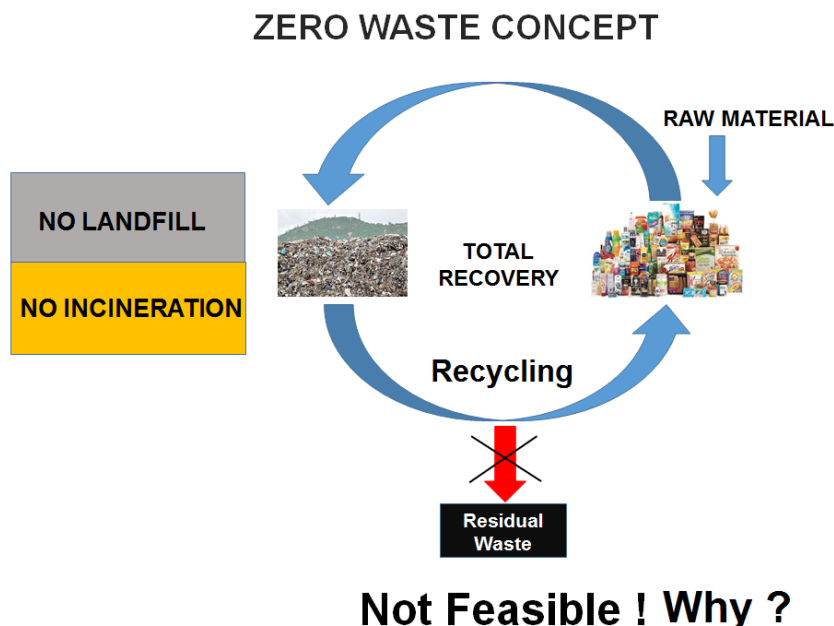


Figure 1.1: Zero Waste Concept

"Zero Waste is a goal that is ethical, economical, and efficient and visionary, to guide people in changing their lifestyles and practices to emulate sustainable natural cycles, where all discarded materials are designed to become resources for others to use." Zero Waste means designing and managing products and processes to systematically avoid

and eliminate the volume and toxicity of waste and materials, conserve and recover all resources, and not burn or bury them. Implementing Zero Waste will eliminate all discharges to land, water or air that are a threat to planetary, human, animal or plant health. Achieving zero waste is often described as the only solution to the world's mounting solid waste problems. Many supporters of zero waste goals believe that the only ways to achieve this are through reduction and complete material recovery (recycling) techniques. However, there are significant practical, economic and other factors that contribute to this issue. This work assesses information on the technical obstacles towards achieving zero waste. Second to organic waste, paper and plastic waste streams are the two largest components of the Municipal Solid Waste stream (MSW). Figure 1.2, shows the percentage breakdown of MSW in the US where paper, plastic, metal and glass combined constitute 53% of the waste stream. Therefore, according to the zero waste theory this 53% should be recycled with total recovery of material. Which has not been yet achieved.

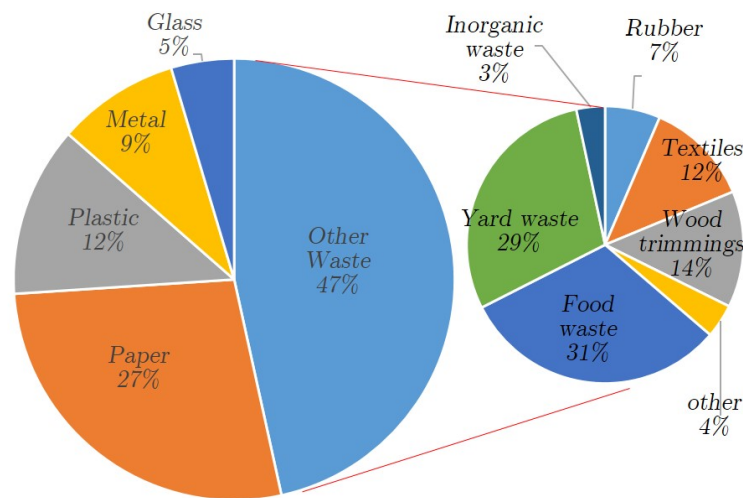


Figure 1.2: Composition of the municipal solid waste stream

Each year, the United States generates a massive amount of municipal solid waste (MSW). Current estimates of MSW generation range from 251 million tons per year to 389 million tons per year [1]. In 2012, over 53.8% of this material was disposed in landfills(Figure 1.3). About 34.5% is recycled and composted and roughly 11.7% is converted into energy through combustion.[2] Although generation rates have stabilized at about 751 kilograms per person per year, increasing population and changing consumer practices have increased MSW generation over the past thirty years by 65.5%. [2] The U.S. has focused much attention on increasing recycling and composting, rates that together they have roughly doubled over the past 20 years from about 16% to about 34%[2]. Recycling of the four major waste streams (paper, plastic, metal and glass) can be improved but still there are certain technical limitations to it which will be addressed in further sections. Increased efforts to recover more material and value from municipal waste has fueled the growth in recycling and composting rates all across the world. However, the role of landfills in waste processing has not diminished, as evidenced by the more than half of the waste still going to landfills in the US. The recycling of waste can be improved significantly but will continue to increase after a certain degree, this will be discussed in

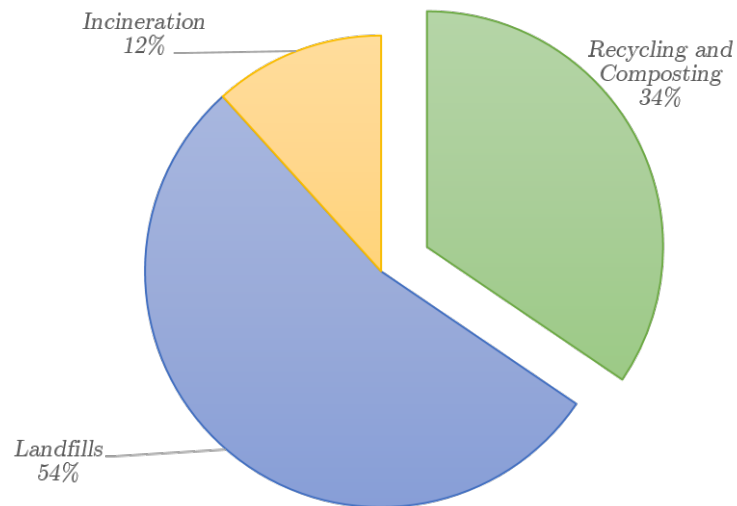


Figure 1.3: Current waste processing strategies in USA. ( Source: EPA annual report 2012)

further chapters. The alternatives for recycling are incineration, pyrolysis for plastics and encapsulation of waste in bricks or concrete etc. Thermal conversion is one alternative which can provide energy as a product and in process reduce the waste volume by a significant amount. Thermal conversion or the controlled combustion reduces the volume of waste by 90%, leaving an ash residue. It is very crucial to make existing processes more sustainable and efficient.

# Chapter 2

## Recycling

### 2.1 Paper Waste

#### 2.1.1 Limitations in Paper recycling

On an average, waste paper constitutes about 20 percent of the municipal solid waste stream in the U.S. An exhaustive search through published data found the highest paper recycling percentage was found for the Lombardia region of Italy at 85 % [2]. Interestingly, in Lee County Florida, which has achieved zero waste to landfill only recycles 59% of paper waste [5].

It can be seen in Table 2.1 that the amount of paper waste present in the waste stream varies around 20%  $\pm$ 5%. Table 2.1 represents the best and worst case scenario. The values in Table 2.1 are few examples, these are paper waste tonnage generated by the community such that there are no exclusions from the waste streams such as any unaccounted intermediate removal of waste during transfer or loss during the entire waste processing cycle. The highest recycling percentage of 85% in Lombardia was achieved by converting the waste paper into pulp to replace virgin pulp which can reduce the cost of raw materials. However, using processed pulp also creates various difficulties while producing paper. These problems and their causes are discussed below. The paper making process is a sensitive and complex process and change in feedstock at any stage may deteriorate the quality of the paper, affecting properties such as tensile strength, brightness, breaking length, density and tear index. Importantly, paper waste collected from a city or a community typically does not contain one type or category. It is a combination of different types that, when converted to pulp, have different impacts on the paper making process and therefore towards recycling.

Cities/ County/ Region, Country (Year)	Total Waste Generated (Tons)	Total paper waste (Tons)	Percentage of Paper waste	Percentage of paper waste recycled
Lombardia, Italy (2009)	4403066	538730	12.2	85
Aarhus, Denmark (2005)	93600	26400	28.2	72
Lee county, Florida, USA (2012)	1098301	145400	13.2	59
Orange county, Florida, USA (2012)	1881650	306582	16.3	58
Sarasota, USA (2012)	719643	107303	14.9	44

Table 2.1: Communities achieving high rates of recycling selected on the basis of amount waste recycled. [5] [4]

Table 2.2 below is an example of how recycling can have different effects on the same property. The tensile index (which is a measure of tear strength) for unbeaten softwood pulp increases by 23 % after recycling twice, but it decreases by 16% for beaten softwood pulp. The two different pulp, beaten and unbeaten, have different cross-sectional area and bonding strength and these properties are influenced after various iterations of recycling. These variations can also affect the strength of the final product. This can also be complicated and entirely unpredictable given the uncertain composition due to collection efficiencies of waste paper.

No. of times Recycled	Tensile Index	Tear Index
<b>Unbeaten softwood pulp</b>		
0	25	16
1	29	19
2	31	18
<b>Beaten softwood pulp</b>		
0	95	8
1	78	11
2	79	10

Table 2.2: Tensile and Tear Index of Pulp as a function of recycle iteration

The fundamental objective for converting waste into pulp is to recycle the fiber. One of the challenges of fiber recycling is managing the stickies (Stickies are slimy clogs which are formed during the paper making process), [3] which is an expected part of recycled fiber. These stickies are formed due to repeated use of recycled pulp. The chemicals such as adhesives, fillers, inks. form the stickies that tend to weaken web strength, reduce paper brightness and paper quality and modify paper texture. [3] Additionally, fiber properties degrade when they are repeatedly subjected to chemical and mechanical treatments and drying. Fibers can be upgraded by refining, adding chemicals and primer fibers which improves the bonding characteristics of fiber, thus improving the strength of the paper. [3] However, it also increases the number of small cellulose fibers, also called fines which are the fraction of solids that passes through a 200 mesh screen, usually 75 microns in size.

[3] Fines are necessary to maintain the strength of paper but an excess of fines can reduce the dewatering rate that is significant when compared to the dewatering rate of virgin pulp, thus lowering the productivity of the paper making process. A trial conducted in a European mill, producing towel and tissue, showed that machine speed increased by 9.3% once the pulp was treated for fines removal. [3] Therefore the paper making productivity is directly related to the quality of the recycled pulp; the lower the quality of pulp, the greater its impact on productivity.

Treatment	Pulp properties		
	Freeness (SR)	Tensile Index (Nm/g)	Tear Index (Nm <sup>2</sup> /Kg)
Untreated	37±0.5	51.4±1.5	10.81±0.49
Enzyme1 (Indi Age SuperL)	31±0.7	52.2±2.2	8.06±0.27

Table 2.3: Effect of enzyme on freeness, tensile and tear index [3]

These fines can be reduced by treating the pulp with cellulolytic enzymes. Yet it is crucial to maintain a proper balance between the amount of enzyme added and strength treatment so productivity is not hindered and pulp quality is maintained. This becomes difficult when pulp quality varies due to the quality of incoming paper, and the enzyme to fines ratio must be tightly controlled. From Table 2.3 it can be observed that the enzyme treatment improved the drainage and tensile properties of pulp but resulted in reduction in the tear index. [3] This may pose a problem when a certain quality of paper is required, thus limiting the usage of the enzyme and ultimately limiting the production speed.

From Figure 2.1 it is observed that increasing the amount of enzyme per tonne of pulp (TP) will have opposing effects as loading increases. The optimal enzyme dosage, for xylanase enzyme treatment is 2-5 international units (IU). However, it is known that the waste paper pulp will continuously fluctuate in consistency, varying in the amount of contaminants present and quality of fiber. These fluctuations can be several order of magnitudes. Such variation has a direct effect on the quantity of fines present in the pulp after refining, and enzyme loading has to be determined based on the quantity of fines, thus making it crucial to control the dosage of enzyme. Figure 2.1 illustrates that a small change in the dosage can cause significant changes in tensile strength.

If the fiber bond strength is too low it will cause the paper sheet to break during various paper processes. Since repeated recycling leads to shorter fibers and eventually more fines, it will weaken the fiber bond strength, which affects the breaking length, shown in Table 2.4. Changes in the quantity of fines can cause paper making processes to have unintentional disruptions, either hindering the process or damaging the product.

Recycle Iterations	0	1	2	4
Breaking length (km)	5.29	4.48	4.36	3.93

Table 2.4: Breaking length as a function of recycle iteration (Sulphite pulp)[6]

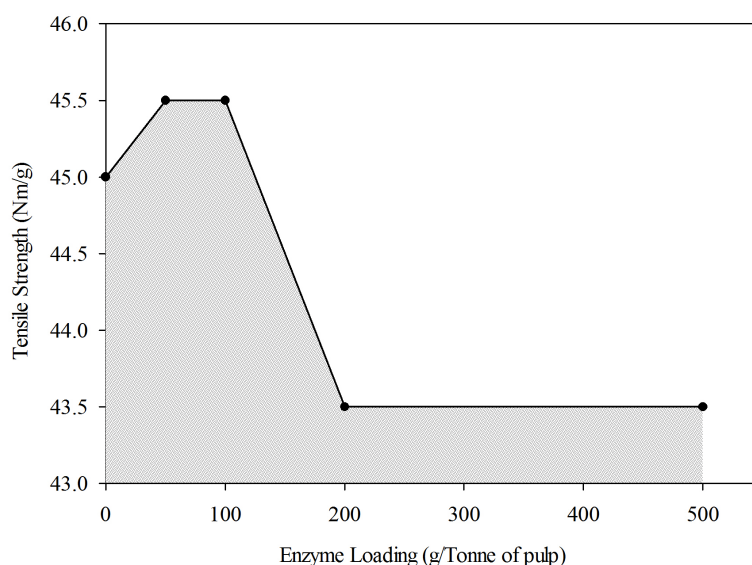


Figure 2.1: Effect of enzyme in grams per tonne of pulp (TP) on tensile strength

Fibers produced from mechanical pulping have lignin which makes stiff and rounded fiber walls, causing weakly bonded fiber sections and thus a low strength virgin paper. Recycling may help in flattening and improving the qualities of these fibers. The complete opposite phenomenon happens when fiber from paper produced through chemical pulping process is recycled. The more flexible fiber from the chemical pulping process produces a strong virgin paper and when these fibers are recycled the fiber walls are weakened and this results in loss of strength in paper produced due to weak fiber bonds. This contrasting behavior of different pulps make it hard to control the strength of recycled paper. The complexity of the problem compounds as waste paper entering recycling facilities contains paper manufactured by various methods. Table 2.4 shows how repeated recycling can affect the breaking length of paper during the process. Breaking length represents tensile strength and webbing characteristics of the paper manufactured.

All methods to improve the quality to match current market standards require large amounts of time and energy, for example, total energy consumption in low-consistency refining process is approximately 30-60 kWh per ton and can be more than 100 kWh per ton if it is a Kraft waste.[3] Low drainage of the pulp also causes higher energy costs, which in this case is related to steam consumption. With proper treatment, steam consumption can be reduced by 6-7%. [3] These limitations do not allow recycling plants to utilize the entire amount of waste paper generated as it is not practical to convert the entire mass into pulp without significantly complicating the process. Utilization of recovered paper in domestic paper mills seems to confirm the limitations to recycling caused by these factors. Those rates have varied from 44.5% to 63.5% (19 to 42.7% increase) over 13

years (2000-2013) and 57.7% to 63.5% (5.8 to 10.05% increase) over 5 years (2008- 2013), as shown by American Forest and Paper Association (AF&PA) annual recovered paper statistics. The annual recovery of paper has been close to 50,000 kilotons ( $\pm 3\%$ ) from 2008 to 2013, but the amount of waste received by facilities for recycling has decreased from 89,838 to 78,954 kilotons. The amount of recovered paper has not grown past 66.4% (in 2011), indicating a practical limitation to the amount of recycled paper domestic mills can incorporate into their production practices. [8]

Type of Waste paper	Garbage weight (kg),G	Recyclables Weight (kg),R	Total waste (kg), (G+R)	Percentage of Material Diverted to Recyclable stream ( $R/(G+R)$ )
ONP (old newspaper)	48.715	287.99	336.71	<b>85.53</b>
OCC (old corrugated cardboard)	62.82	218.67	281.49	<b>77.68</b>
Mixed Paper	470.01	359.06	829.07	43.31
Food Contaminated Paper	234.64	16.23	250.88	6.47
<b>Total</b>	<b>816.19</b>	<b>881.97</b>	<b>1698.17</b>	<b>51.94</b>

Table 2.5: Waste Characterization data for different types of paper waste (2014) [9]

Scenario	1		2	
	Single Processing	Stream MRF & Recovery	Single Processing & Recovery, MWPF for MSW and MRF residue	Stream MRF
	Est. % Recyclables Recovered at MRF	Total Recovery Rate, Recyclable Materials	% Recovered at MWPF from Garbage and MRF Residue	Total Recovery Rate, Recyclable Materials with MRF + MWPF
OCC	85%	66%	65%	88%
Mixed Paper	85%	37%	50%	68%
ONP	90%	77%	50%	88%
<b>Total</b>		<b>52%</b>		<b>77%</b>

Table 2.6: Recovery Estimates for Paper in Processing Facilities (2014) [9]

This point is underscored by what happens in the intermediate step between collection and delivery to a mill, at a single stream recycling or mixed waste processing facility where paper is segregated from other recyclables. The sample data analyzed is from a community presented in Table 2.5 and shows how a big improvement can be made in the



food contaminated paper category. Table 2.6 shows two sample processing scenarios for OCC (Old Corrugated Cardboard), Mixed Paper, and ONP (Old Newspaper) generated from residential sources using data from Table 5 a). Scenario 1 shows typical recovery rates at a single-stream materials recovery facility (MRF), and the resultant recovery rate of materials from the overall waste stream (recyclables source separated and those that were placed in the garbage). Scenario 2 shows the resultant recovery rate from the overall waste stream if there is additional recovery of these materials from the garbage and MRF residue through use of a mixed waste processing facility (MWPF). Even through typical processing with modern sorting technologies, it is estimated that only up to 77% of these recyclable materials can be separated from the overall waste stream. Such limitations reduce the possibility of a true "closed loop" recycling system for paper. There must be a continuing fresh input of primer fibers into the paper making system to allow the proper balance of fiber and maintain the integrity of the product.

## 2.2 Plastic Waste

### 2.2.1 Limitations in Plastic recycling

Since the beginning of mass production of plastics in the 1940s, plastics have become an integral part of day to day life. However, this also has resulted in a huge increase in the presence of plastics in municipal waste streams. The contribution of plastic in waste streams can vary from 2% to 20%. This large deviation is due to the variety of policies implemented by communities to minimize the usage of plastic and to maximize its source separation for recycling. The average recycling rate of plastic remains at 40% of the generated plastic stream per annum. Table 2.7 presents data from selected regions of the U.S., and includes the Lombardia case as a comparison. The available data given in Table 2.7 on waste recycling in Florida for plastics, shows that Lee County has a high recycling percentage at 87% (4,942 Tons), for plastic bottles, while other counties have around 40% or lower. Orange County also has a high percentage recycled for other plastic streams at 76% (12,308 Tons).

For example, Polypropylene and High density polyethylene have densities 946 kg per  $\text{m}^3$  and 970 kg per  $\text{mm}^3$ . However, density of polyethylene terephthalate is 1380 kg per  $\text{m}^3$  and polyvinyl chloride has densities ranging from 1320 -1420 kg per  $\text{mm}^3$ , which causes one of the two polymers to end up in the others' polymer stream during sorting. This is a fundamental problem to increasing the effectiveness of density media separators. [11] As a result, the system directs more desired material into the residual stream, which helps explain why the recovery of plastics stands at approximately 50- 60% globally.

Polymers such as polyethylene terephthalate (PET), polypropylene (PP), polyethylene (PE), and polystyrene (PS) are some of the common polymers present in the waste stream. The effects on tensile and impact properties of a PP-PE blend were studied by R. Strapasson. [12] The two important properties of a polymer which defines its application are elastic modulus and impact strength. Elastic modulus is a number that measures the ability of a substances to deform elastically when a force is applied to it. Impact strength is the capability of the material to withstand a suddenly applied load. Figure 2.2 shows that the elastic properties of the mixture decrease with the increase in

Cities/ County/ Region, Country (Year)	Total Waste Generated (Tons)	Total Plastic waste (Tons)	Plastic waste (%)	Waste Fraction				Percentage waste recy- cled		
				Plastic bottles	Other plastics	Plastic bottles	Other plastics	Plastic bottles	Other plastics	Total
Orange County, Florida ,USA (2012)	1,881,650	17,859	0.9	9.35	90.64	44	76			73
Lombardia, Italy (2009)	4,403,066	127,283	2.8	NR	NR	NR	NR			48
Lee County, Florida ,USA (2012)	1,098,301	17,594	1.6	32.20	67.79	87	16			39
Indian River County, Florida ,USA (2012)	245,811	7,837	3.1	34.75	65.24	49	16			27
Putnam County, Florida ,USA (2012)	[9]80,097	6,118	7.6	26.57	73.42	54	1			15
Sarasota County, Florida ,USA (2012)	719,643	44,501	6.1	16.68	83.31	49	4			12

Table 2.7: Communities selected on the basis of amount waste recycled (Plastic) [5] [4]

Polymer	% of Separation from waste stream
Polypropylene (PP)	96
Polyethylene (PE)	94
Polyethylene terephthalate (PET)	94
Polystyrene (PS)	87

Table 2.8: Experimental values for polymer separation from waste stream by NIR sensors [11]

PE weight % in the PP/PE mixture, but a contrasting effect is observed with the impact properties of the same mixture. For a 10 wt. % increase of PE in the PP/PE mixture, elastic modulus of the mixture decreases by an average of 10.38% of initial modulus, but impact strength increases by 30%. From Figure 2.2 it can be seen that a simple two component mixture can have opposite trends of the two main properties of plastics. With the increase in PE, as a potential contaminant plastic polymer, elastic modulus of the blend decreases dramatically. However, the impact strength of the blend increases. These properties are crucial in understanding the effects of contamination in a pure polymer stream by another polymer as they determine the quality of the final product. [4][5]

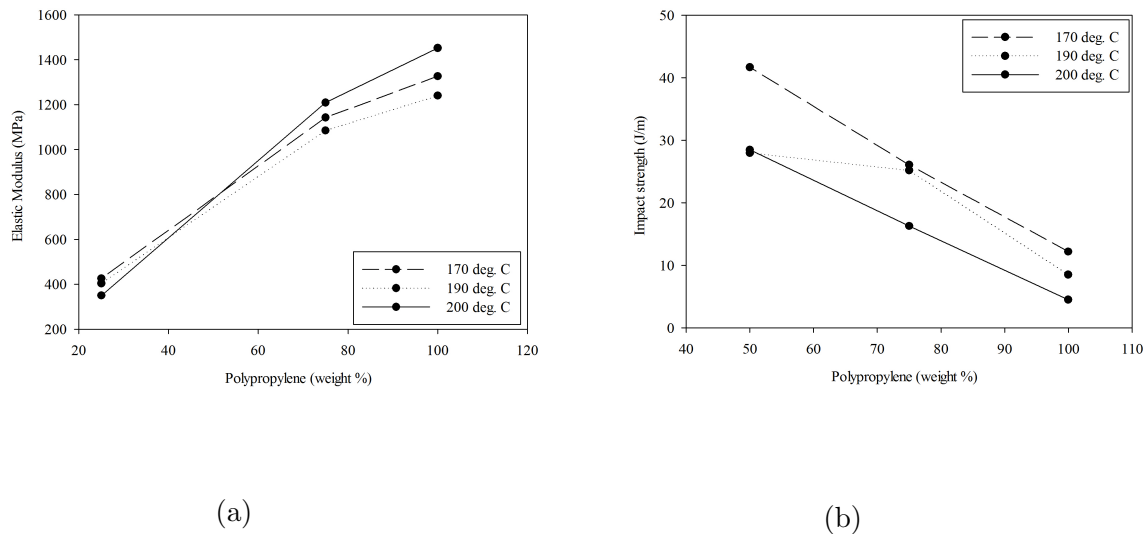


Figure 2.2: Effect of PE contamination in PP stream on (a) Elasticity and (b) Impact properties. [6]

A linear dependency can be seen for elastic modulus with respect to the injection temperatures. The trend for the impact strength and injection temperature is complex, thus making it difficult to manage the waste and obtain a desired property for the final product if multiple contaminants were present in the same mixture. It is vital to understand that unlike the controlled composition of the experiment with two polymers in Figure 2.2, the actual waste stream contains a wide range of polymers. This wide range of contamination of polymers can alone result in extreme and unpredictable changes in properties of the polymer/plastic blend greatly impacting the final market acceptance and value.

Addition of modifiers to improve the impact properties of the plastic blend is a common practice. Effects of the addition of impact modifiers are shown in the Figure 2.2. The blend used in the test shown is a blend of Polycarbonate (PC) - 60 wt. %, Polycarbonate/Acrylonite - butadiene - styrene (PC/ABS) -20 wt. %, Acrylonite - butadiene - styrene/High Impact polystyrene(ABS/HIPS) - 10 wt. %, and Acrylonite - butadiene - styrene (ABS) - 10 wt.%. [13] The addition of 5 wt% of virgin polycarbonate (VPC) improved both tensile and impact properties of the blend but when this is increased to 10 wt% the tensile strength began to decrease. An increase in polycarbonate concentration improves interfacial adhesion between polycarbonate and polystyrene, thus improving the tensile and impact properties of the blend (Figure 2.3). However, further addition of the VPC gives an opposite effect. To improve the impact properties further, impact modifiers are added to the blend. [13] However, after a certain quantity of impact modifier addition, in this case 15 wt%, the tensile and impact properties both start deteriorating. Thus, making it necessary to identify an optimum addition quantity to blend so that the final polymer product properties are maintained in a desired range to yield a product with desired, engineered quality. Therefore, this parameter adds a complication to the recycling potential of plastics. That is, if the stream composition changes, the addition of the modifier must change. Since it is difficult to obtain a continuous characterization of the the plastics mix coming into the facility, the necessary adjustments in modifiers is difficult. Restricting the extent of plastics waste processed.

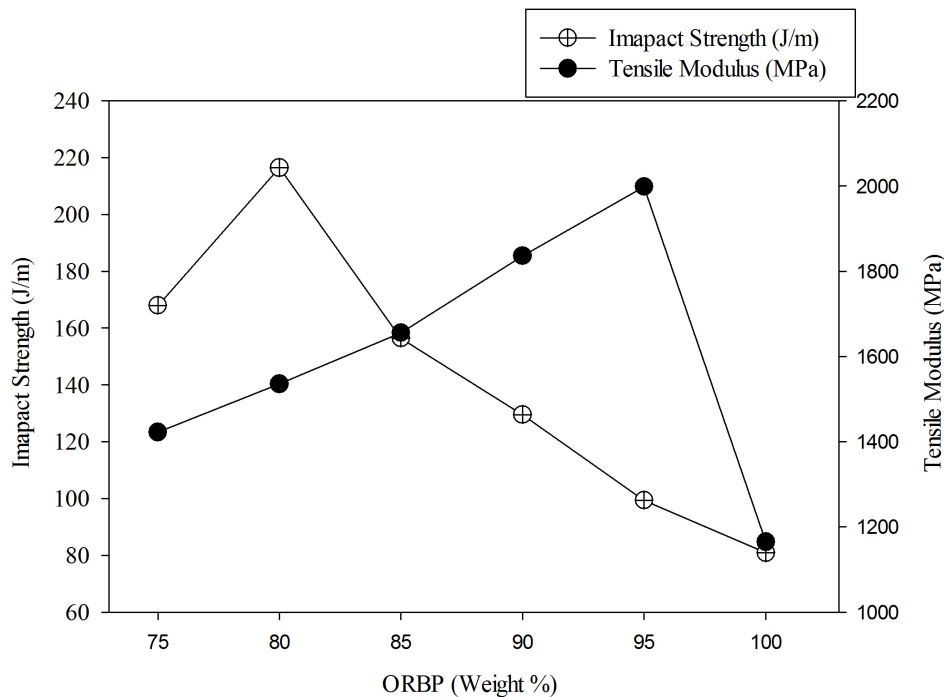


Figure 2.3: Effect of Impact modifier on recycled blend plastic (ORBP - Optimal Recycle Blend Plastic, VPC - Virgin Polycarbonate, IM - Impact modifier) [13]

The selection of the modifiers depends upon blend composition requiring a very good approximation of the concentration of polymers in the waste stream, which is a difficult task given the wide range of polymer and polymer mixes present. This creates complications during the plasticizing of the polymers, if the impurities in the recycled polymer blend increase or the blend composition changes, then the melt flow index (MFI), which is measure of the ease of flow of polymer, may change to unacceptable levels. Good MFI ensures smooth operation of the process such intrusion and molding. However, good MFI is correlated to good compatibility of polymers. One major challenge for producing recycled resins from plastic waste is that the different types of plastic are not compatible with each other, primarily because of the inherent immiscibility at the molecular level and differences in processing requirements at a macro-scale. For example, a small amount of PVC contaminant in a PET recycle stream will degrade the recycled PET resin, owing to evolution of hydrochloric acid gas from the PVC. The nominal process temperature for PET manufacturing is 2850 °C, however for PVC it is 1900 °C. Conversely, PET in a PVC recycle stream will form solid lumps of undispersed crystalline PET, which significantly reduces the value of the recycled material.

Table 2.9 shows the amount of recyclables collected during a waste characterization conducted among the same 484 houses presented in Table 2.5. The highest percentage of total recyclables present in the recycling stream is HDPE (High density Polyethylene) at 71.61%, and the lowest is bag and Films at 19.90%. HDPE can be processed at higher temperatures, above 2000 °C. This makes it highly recyclable as it does not degrade easily when subjected to high temperatures, which in the case of bags and films is not possible because they degrade near temperatures of 100 °C and will char at temperatures near 500 °C. It is clear these limitations will not allow for 100% recycling of plastics unless the streams are composed of only one type of resin. Since many plastic products contain multiple types of resins for consumer performance goals, streams of discarded plastic products cannot contain one resin category.

Types of Plastic waste	Garbage weight (kg),G	Recyclables Weight (kg),R	Total waste (Kg), (G+R)	Percentage of Material Diverted to Recyclable stream (R/(G+R))
PET	133.76	127.15	260.92	48.73
HDPE (natural)	22.40	56.51	78.92	71.61
HDPE (colored)	53.11	73.20	126.32	57.95
Mixed Plastic	220.80	98.06	318.87	30.75
Bags& Film	249.24	61.91	311.16	19.90
Total	679.34	416.86	1096.2	38.03

Table 2.9: Waste Characterization data for plastics (2014)

Scenario	1		2	
	Single Stream MRF Processing & Recovery		Single Stream MRF Processing & Recovery, MWPF for MSW and MRF residue	
	Est. % Recyclables Recovered at MRF	Total Recovery Rate, Recyclable Materials	% Recovered at MWPF from Garbage and MRF Residue	Total Recovery Rate, Recyclable Materials with MRF + MWPF
<b>PET</b>	90%	44%	85%	92%
<b>HDPE (natural)</b>	90%	64%	85%	95%
<b>HDPE (colored)</b>	90%	52%	85%	93%
<b>Mixed Plastic</b>	80%	25%	75%	81%
<b>Bags&amp; Film</b>	20%	4%	30%	33%
<b>Total</b>		29%		72%

Table 2.10: Recovery Estimates for Plastic in Processing Facilities (2014) [9]

Further difficulty in separation and then processing leads to rejecting the undesirable plastic waste. Table 2.10 shows two sample processing scenarios for plastics generated from residential sources. The sample data analyzed is from the community presented in Table 2.9. Scenario 1 shows typical recovery rates at a single-stream MRF, and the resultant recovery rate of materials from the overall waste stream (recyclables source separated and those that were placed in the garbage). Scenario 2 shows the resultant recovery rate from the overall waste stream if there is additional recovery of these materials from the garbage and MRF residue through use of a mixed waste processing facility (MWPF).

Even through typical processing with modern sorting technologies, it is estimated that only up to 72% of these recyclable materials can be separated from the overall waste stream. A closed loop recycling system is possible for a certain classes of plastics, however, given that the waste stream is heterogeneous, the actual implementation of a closed-loop system seems highly improbable. It is possible to blend different polymers into one product and add modifiers to improve the properties of the blend. For example, the Polycarbonate - Acrylonite-butadine-styrene blend whose tensile properties changed with contaminate amount. However, there will always be certain classes of polymers that can never be paired together and will have to be managed using other strategies, making it impossible to reach zero waste targets by material recovery alone.

## 2.3 Metal Waste

### 2.3.1 Limitations in Metal recycling

The contribution of metals in waste stream can vary from 5% to 25%. They can be divided into two groups such as ferrous and non-ferrous. The recycling rates for metals are found to be high because they are easier to separate and they are more valuable than plastics and paper. Metal recycling is seen as most profitable, as a result the communities which are dedicated towards metal recovery from MSW waste, achieve high recycling rates. Such as, Polk County, Florida has one of the high efficiencies in the region for recovering metals from waste stream at 94% leaving 5966 tons of residue metal waste yet to be processed. The 5966 tons of residue is mainly due to failure in separating metal and other components such as plastics, semiconductors and many more electronic components. Separation of metals from other components or in simple words disassembly of these components is very difficult. Although augmenting the sorting and separation of waste stream can increase the recycling process efficiency but even after these optimizations the efficiencies can never reach 100% due to thermodynamic and other limitations (Castro 2004).

The metal waste stream consists of a lot of contaminants in various forms, most of them are cleared out during the cleaning process. After which it is sent to recycling plants but the impurities present in form of alloys or from other components such as semiconductors or electronic parts are also present in the mix. These elements are hard to separate but are also valuable as these elements can range from germanium, gold, platinum to aluminum, boron and copper. Recycling process for metals follows a similar path as to metallurgical operations for extraction of pure elements from ores. When an alloy is desired the pure melt is mixed with a fixed amount of other impurities which are specific to the alloy being produced. So, when metal waste is added to the melt it increases the amount of impurities and this causes a change in metal composition and increases the cost of processing. Impurities can cause failure of the final product by changing its physical and mechanical properties. It can additionally cause process complications such as high dilution requirements, higher operating temperatures, or loss of desired elements.

Impurities present in the mix may or may not reduce to pure elements depending on their standard Gibbs energy value. Carbon is used in many metals processing routes as a reducing agent. The reduction of oxides with carbon occurs by supplying carbon that reacts with the oxygen from the oxide, forming CO and CO<sub>2</sub>, and a reduced metal is obtained. Graphically, the reduction of the metal will occur to the right of the point where the carbon and the metal oxidation lines cross, and thus  $\Delta G_0$  will be negative for the sum of all reactions. It can be seen on Fig. 2.4 that at temperatures higher than about 750 °C, FeO will be reduced by carbon to Fe, and that Cu<sub>2</sub>O can be reduced at temperatures above 100 °C. The reduction of oxides of reactive metals such as aluminium, magnesium and titanium occurs only at very high temperatures for above the respective melting points of the metals, and the reduced metals would therefore reduce very easily when even small amounts of oxygen are present. When a recycling plant tries to recover iron from the waste it operates at about 1230 °C in the smelting chamber, at this temperature iron and the impurities with such as aluminum and copper have different free energies which effects the reduction of these metals to pure form. For example they are present in the form of oxides, for iron reduction  $\Delta G_0 = -68 \text{ KJ (mol O}_2^{-1})$ , for copper  $\Delta G_0 = -284 \text{ KJ}$

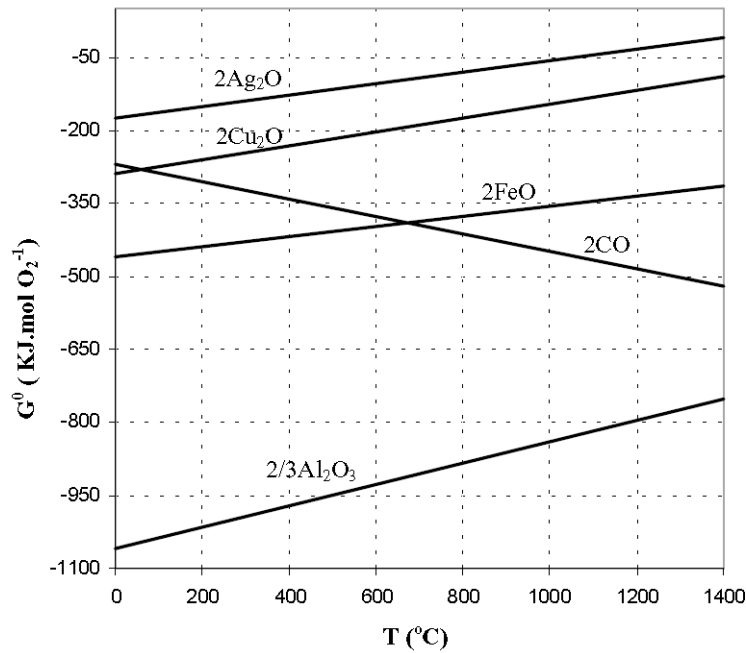


Figure 2.4: Extract of the Ellingham diagram for some oxides [7] [8]

(mol  $O_2^{-1}$ ), and for aluminum it is  $\Delta G_0 = +715$  KJ (mol  $O_2^{-1}$ ). From these values it can be concluded that aluminum will remain in the form of alumina and will be lost as slag and copper will remain dissolved in the molten iron solution. Now this impure copper is carried out in to the further stages. The highly impure stream, copper contamination in iron, start creating issues. The final product after recycling the scrap metals must have a certain property for further use, such as specific strength for construction or flexibility for wires. In order to have these consistent properties the recycled product should have impurities within the admissible limits. High percentage of impurities will require the smelter to add more pure element into the molten stream so as to dilute the impurities. As in our above case where copper is the impurity let us assume that the stream has 0.7% Cu and alloy has a copper limit of 0.5% , so to dilute the impurity pure iron needs to be added which also contains some impurities. Supposing the primary iron contains 0.25% of Cu, a simple calculation indicates that 400 kg of pure iron is required to dilute 1000 kg of scrap. Approximately 40% of the initial scarp weight needs to be added to improve the quality of the product which is obviously costly for the smelter and thats why rejection of amount of the waste is more profitable than including it into the stream.

## 2.4 Glass Waste

### 2.4.1 Limitations in Glass recycling

After metals glass is one of the most recycled material as waste glass saves a lot of energy when added to glass production. Out of the areas observed for the extent of recycling carried out, Lombardi, Italy had the highest recycling percentage at 91%. The method used by this region for recycling was to convert glass cullet to generic glass container. Even after recycling 91% waste glass collected they are left with 32783 metric tons of waste glass. This residue stream mostly consist of the glass with high contamination,



such as colored glass ceramic glass metals etc.

Cullet specifications	Acceptable cullet (unit in mass % or grams/ ton cullet)
Stones, ceramics, chinaware, pottery excluding glass ceramics	<25-35 g/ton
Glass ceramics Indicative	<25 g/ton
Glass ceramic pieces If present size should be	< 3-4 mm
Magnetic metals	<5 g/ton
Non-magnetic metals	<5g/ton
Lead	<1 g/ton
Aluminum	< 5 g/ton
All Metals	< 7 g/ton
Organic material	<200 or 500 g/ton
COD of washing water from cullet	<1200 -1500 mg O <sub>2</sub> /liter
Plastics	< 60 g/ton
Moisture	<2-3% (preferred)
Paper/cork/wood	<1500 g/ton
Opal glass	<100 g/ton
Grain cullet size	No cullet pieces >7cm Cullet pieces <0.5 cm; max 12%

Table 2.11: Glass specification for recycling

While recycling glass the companies have a specific and strict requirements for the waste stream coming in, Table 2.11. the presence of contaminants in the stream can cause severe problem in the glass manufacture processes. Highly polluted cullet streams with ceramic particles which do not melt or completely dissolve can cause fracture in the glass product. High glass ceramic content can cause damage to shear blades of the gobbing system, which can interrupt the gob delivery process to the forming machines and as a result interruptions in production. So, these kind of contaminations should be removed. Not only the process is hampered but contaminants can also start damaging refractory, one such case is caused when high amounts of lead impurities are present. The reduced lead will sink to the tank bottom and there it will attack the refractory, this is also called downward drilling. Various contaminants cause different effects, iron sulfates causes formation of cords, nickel or stainless steel flakes may form small NiS inclusions which can be a severe problem for float glass production.

In order to avoid these defects and maintain the quality of glass produced the recycling plants need to sort the stream efficiently and during this a lot of usable glass is also separated. But this is necessary as the defected product will be rejected during the inspection period and add on to the losses. A general cullet specification for recycling

cullet into glass containers is shown in the table below and if the cullet does not meet these specifications then it is rejected.

## 2.5 Residual Waste

Improvement in recovery is restricted by the various performance limitations present throughout the associated processes. The amount of fines in waste paper pulp is to a degree a controlling factor in the waste paper recycling. Fines define the treatment and intensity of treatment needed. Excess or lack of fines can change the consistency of pulp, thus increasing the process cost by increasing the energy requirement or decreasing the strength of the paper manufactured. Also, the process is affected by the number of times fibers were recycled. In order to bring the recovery extent to 100%, it is necessary to recover materials from all sub-waste streams, Old newspaper to food contaminated paper. However, fiber quality in these various waste streams vary a lot, making it unmanageable to include all sub-waste streams. Ultimately leaving significant amount of paper waste to be processed further by other methods.

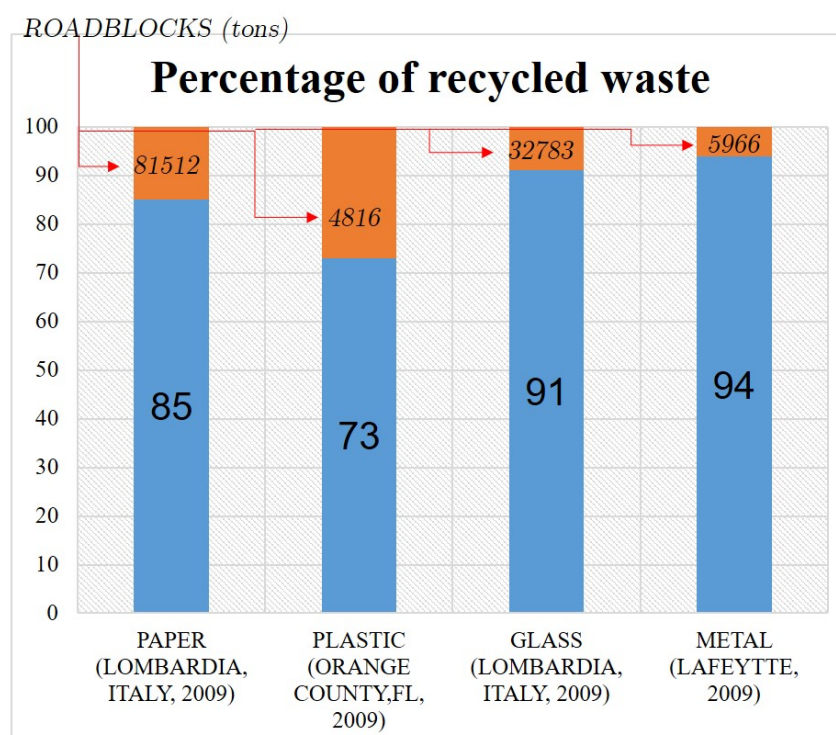


Figure 2.5: The optimum recovery achieved by different communities for different waste streams.

Plastic recovery primarily depends on the separation or sorting of the polymers before processing. Recycling of plastics is most effective when closed-loop recycling can be done for different polymers as it allows to retain the initial properties. However a plastic waste stream consist of large number of different polymers and separation of different polymers into individual polymer steams is necessary to recycle them, as contamination by other polymers will affect the final properties of the product formed. This is a major limitation in plastics recycling, as even with small throughput of 3 tonne per hour and

there is still 5% contaminant remaining in the stream. This 5% contaminate can either improve or deteriorate the quality of the mix depending on its compatibility with other polymers present in the stream. This restricts use of highly contaminated waste polymer streams for recycling. Thus making it difficult to recycle the complete plastic waste stream and achieve zero waste target. Which is complete recovery without landfill and waste incineration for energy. With current technologies it is possible to reach 85% of recovery of paper and 79% of recovery for plastics, as seen in above mentioned cases. Given the current technical limitations of recycling of the various waste stream components described above, it will be a difficult task to achieve zero waste target without other strategies. Therefore, it is crucial to add other strategies to achieve the zero waste target.

If we are to consider an ideal community, where paper and plastic generation (Figure 2.5) and recovery amounts are matched with the above mentioned individual cases, there will still be at least 86,117 tons of waste left in our ideal community, which is 15.36% of the paper and plastic waste stream combined. **Although material recovery of 84.63% would be a definite improvement over the current statistics, 15.36% of residual waste translates into 17.23 million tons of waste per year in the U.S., from only two waste streams.** This is in addition to residual waste from other streams that will be left after optimum material recovery.

## **Part II**

# **WASTE TO ENERGY FACILITIES**

# Chapter 3

## Waste to Energy Facilities

### 3.1 Overview

Chapter 2 clearly shows how complete recovery of materials from Municipal Solid Waste (MSW) can never be achieved with the current technology available for recycling. Therefore, it is necessary to identify additional methods to process the waste so that a community free of waste disposal issue can become a reality. In the absence of new methods, making an existing method more sustainable is our only choice. The other major ways through which waste is currently processed is sending them directly to landfills or first to waste to energy facilities and then sending ash to landfills. Diverting waste to WtE and then sending the ash produced to landfills will reduce the volume of waste by 90%. Therefore reducing 17.23 million tons of waste from paper and plastic waste streams to 1.73 million tons per year, after optimal recycling of 84.63% . This is the best case scenario which can be achieved if recycling is carried at maximum. A waste to energy facilities uses MSW as fuel and thermally converts MSW to obtain heat which is then converted to electricity. Therefore, the only hurdle remaining is to make the residue (ash) from WtE facilities less leach-able or more stable, for it become more feasible and sustainable option.

Fly ash, not the bottom ash, from waste incinerators can be termed as hazardous waste as they contain heavy metal oxides and chlorides which can leach in an acidic or aqueous environment. Disposing ash to landfills without proper treatment can cause leaching of the heavy metals to soil and poisoning, thus creating an environmental hazard. In addition to sending ash to landfills, ash can also be used in various applications. These applications can range from using ash as a pozzolanic material (materials which will react to form cementitious material), or as a filler in construction material such as bricks or ceramics, or as absorbents in waste water or effluent treatment, or as soil stabilization. In order to dispose ash safely or use them, it is crucial to understand the behavior of ash under a leaching environment. Thus a proper characterization of ash was carried out to engineer an appropriate method to solve problem of ash leaching. The main focus of this part of Thesis is to understand the parameters effecting the varying leaching behavior of ash from different sources. The ash contains many toxic heavy metals. However, to simplify the problem only one toxic element is considered, i.e. lead.

## 3.2 Experimental Methodology/Techniques

In this study only the elemental and micro-structure of the bottom ash were investigated with focus on understanding leaching behavior. The marker chosen for the performance of bottom ash was the TCLP (Toxicity Characteristic Leaching Procedure) test value of Lead ( $Pb = 82$ ). The TCLP values obtained for the ash were acquired by using EPA method 1311 [9]. Understanding and deducing the relation between ash morphology, composition and leaching characteristics was the primary objective of performing these experiments.

### 3.2.1 Sample preparation

The bottom ash acquired from seven waste to energy facilities A, B, C, D, E, F and G, were each segregated into two different categories on the basis of size of the ash particles. Particles with size greater than 3/8 inches (9.525 mm) were denoted as large particles and particles with size less than 3/8 inches (9.525 mm) were denoted as small particles. The samples were thoroughly mixed and dried at 100 degree Celsius for 24 hours. The mixed sample was then divided into five 2 grams section for various characterization analysis. In the table 3.1 ash from different sites are shown. The mechanical strength of the particles was not measured using any specific instrument. Particles which would crumble by a simple pinch action after they have been separated are classified as easy to crush particles. It was not in this study scope to test mechanical strength and it's effects.

Sample ID	Mechanical strength	Size Classification
AL	Hard to crush	Particle size greater than 3/8 inches (9.525 mm)
AS	Easily crushed	Particle size less than 3/8 inches (9.525 mm)
BL	Hard to crush	Particle size greater than 3/8 inches (9.525 mm)
BS	Easily crushed	Particle size less than 3/8 inches (9.525 mm)
CL	Hard to crush	Particle size greater than 3/8 inches (9.525 mm)
CS	Easily crushed	Particle size less than 3/8 inches (9.525 mm)
DL	Hard to crush	Particle size greater than 3/8 inches (9.525 mm)
DS	Hard to crush	Particle size less than 3/8 inches (9.525 mm)
EL	Hard to crush	Particle size greater than 3/8 inches (9.525 mm)
ES	Hard to crush	Particle size less than 3/8 inches (9.525 mm)
FL	Easily crushed	Particle size greater than 3/8 inches (9.525 mm)
FS	Easily crushed	Particle size less than 3/8 inches (9.525 mm)
GH	Easily crushed	Particle size greater than 3/8 inches (9.525 mm)
GL	Hard to crush	Particle size greater than 3/8 inches (9.525 mm)
GS	Easily crushed	Particle size less than 3/8 inches (9.525 mm)

Table 3.1: Ash particles classified based on their sizes and hardness

Three main analytical techniques were used X-ray powder diffraction spectroscopy (XRPD), Scanning electron microscopy/ Electron dispersive spectroscopy (SEM/EDS) and

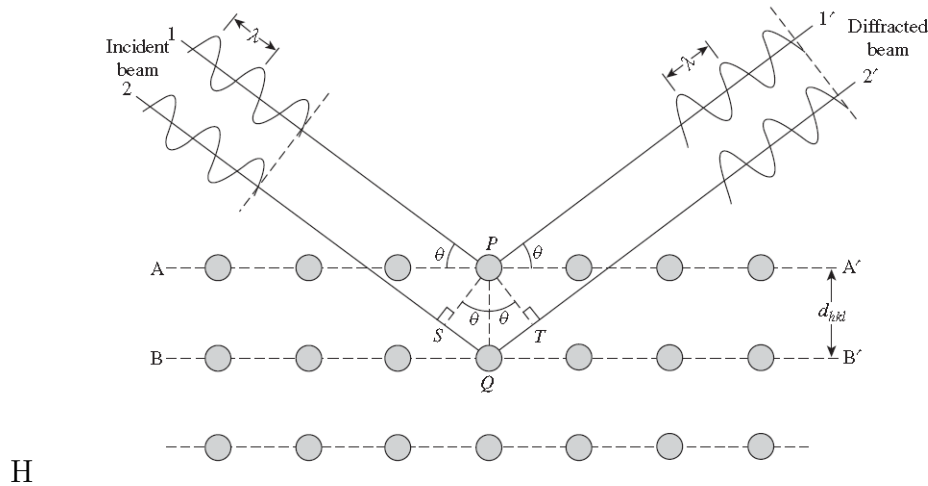


Figure 3.1: Bragg's Law

Inductive coupled plasma spectroscopy (ICPS). SEM/EDS was used to study the microstructure and elemental composition of the ash particles which would help in understanding the morphology of the particles. XRPD was used to identify the compound species and determining their effects on the leaching behavior based on the reactivity of the compounds. However, the dissolution behavior of the ash particles under acid was the main emphasis of the study and this was determined by subjecting ash to accelerated acid attacks and analyzing the leached solution by ICP.

### 3.2.2 X-Ray powder diffraction spectroscopy (XRPD)

X-Ray diffraction spectroscopy, this technique is primarily used to identify the crystalline compositions and structure of a given sample. The technique is based on the Bragg's law. X-rays are electromagnetic waves, as are visible light, but the X-ray wavelength is much shorter than visible light, only in the order of 0.1 nm. X-ray diffraction methods are based on the phenomenon of wave interferences. Two light waves with the same wavelength and traveling in the same direction can either reinforce or cancel each other, depending on their phase difference.[10]

When they have a phase difference of  $n\lambda$  ( $n$  is an integer), called 'in phase', constructive interference occurs. When they have a phase difference of  $n\lambda/2$ , called 'completely out of phase', completely destructive interference occurs. X-ray beams incident on a crystalline solid will be diffracted by the crystallographic planes as illustrated in 3.1. Two in-phase incident waves, beam 1 and beam 2, are deflected by two crystal planes (A and B). The deflected waves will not be in phase except when the following relationship is satisfied.  $n\lambda = 2d\sin\theta$  [10] This equation is the basic Bragg's Law. Bragg's Law can be simply obtained by calculating the path differences between the two beams in 3.1. The path difference depends on the incident angle ( $\theta$ ) and spacing between the parallel crystal planes ( $d$ ). In order to keep these beams in phase, their path difference ( $SQ + QT = 2d\sin\theta$ ) has to equal one or multiple X-ray wavelengths ( $n\lambda$ ). We are able to obtain information on the spacing between atomic planes of a crystal when constructive interference is detected at a given incident angle and a wavelength of the incident beam, based on Bragg's Law. Knowing the spacings of crystallographic planes by diffraction methods,

we can determine the crystal structure of materials. Using this principle a diffraction pattern can be obtained by scanning the sample over a range of angles. Every crystalline compound has unique diffraction pattern, by comparing the obtained diffraction data to the diffraction pattern data from a standard database, compounds present in the ash can be identified. [10]

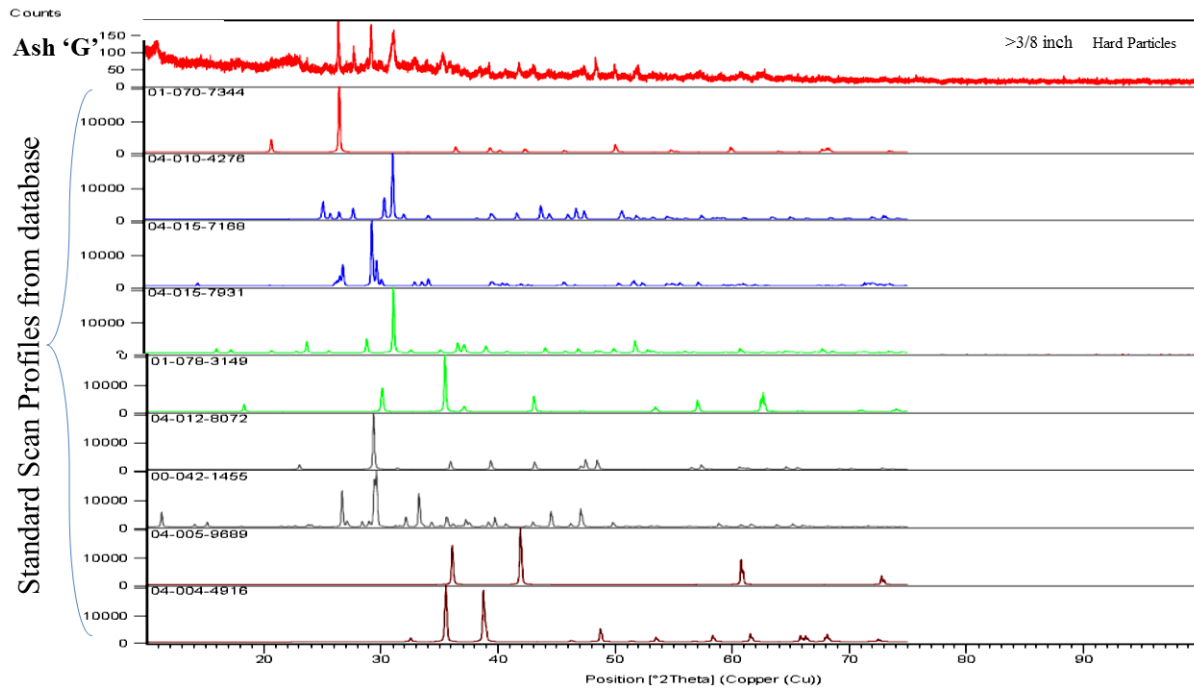


Figure 3.2: XRD profiles of sample with standard scans of matched compounds

Ref. Code	Compound Name	Chemical Formula	Score	Scale F...	SemiQu...
04-012-8072	Calcite, syn	$\text{Ca}(\text{CO}_3)$	23	0.892	6
01-078-3149	Magnetite	$\text{Fe}_3\text{O}_4$	11	0.331	10
01-070-7344	Quartz	$\text{SiO}_2$	10	0.561	4
04-010-4276	Calcium Carbide	$\text{CaC}_2$	6	0.510	5
04-015-7168	coesite	$\text{SiO}_2$	5	0.569	17
04-015-7931	gehlenite, syn	$\text{Ca}_2\text{Al}_2\text{SiO}_7$	13	0.641	7
00-042-1455	Calcium Silicate Chloride	$\text{Ca}_2\text{SiO}_3\text{Cl}_2$	10	0.816	49
04-005-9689	wustite	$\text{FeO}$	10	0.135	1
04-004-4916	Tenorite	$\text{CuO}$	5	0.230	1

Figure 3.3: Matched compounds list from figure 3.2 with reference numbers and quantifications

The major requirement for the XRPD is that the sample should be dry and powdered. Therefore, the ash samples were ground to a aggregate particle size of  $<0.4$  mm. Followed by drying at 60 degree Celsius for 5 hours. These samples were than tested on a Pananalytical XRPD instrument with a scan cycle of 30 minutes for each sample. Figure 3.2 and 3.3 are an example of results obtained form typical sample scan. Figure 3.2 is XRD scan graph with x-axis  $2\theta$  (incident angle) and y-axis is the signal counts at the representative  $2\theta$ . The example shown is for the ash from source G and the successive



scans are the simulated scan from the ICDD (International Crystallography Diffraction Database), these are obtained from the standards and can be used as references to match. Figure 3.2 is the list of the matched compounds for Figure 4.6 which is shown later in the discussion section with references codes and chemical formulas. Data is collected by performing three runs for each sample and then each data set was analyzed separately and then compared for consistency.

### 3.2.3 SEM/EDS

SEM (Scanning electron microscopy) was used to study the micro-structure and surface morphology of the ash samples. SEM coupled with EDS (Electron Dispersive Spectroscopy) was used to identify the basic composition of the ash in addition to information on the probable composition. A scanning electron microscope consists of an electron gun and a series of electromagnetic lenses and apertures as shown in Figure 3.4. In an SEM, the electron beam emitted from an electron gun is condensed to a fine probe for surface scanning. Advanced SEM systems use a field emission gun because of its high beam brightness. Beam brightness plays an even more important role in imaging quality in an SEM. The acceleration voltage for generating an electron beam is in the range 1-40 kV.

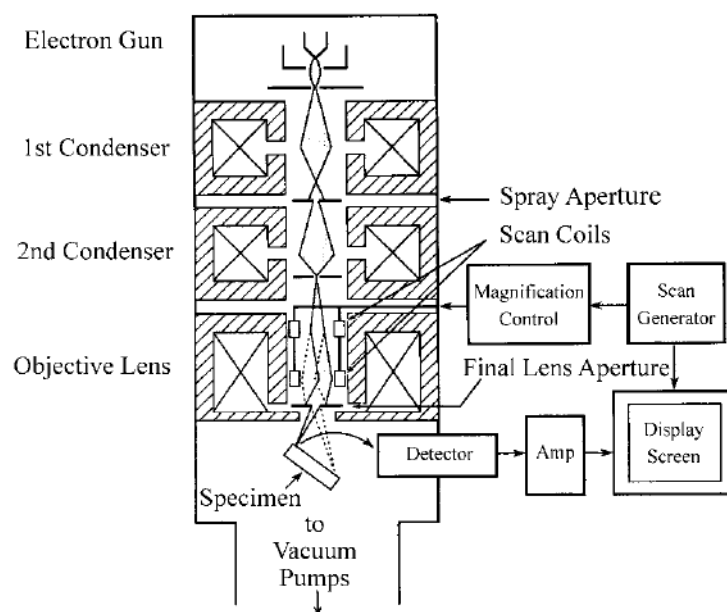


Figure 3.4: SEM schematic

Probe scanning is operated by a beam deflection system incorporated within the objective lens in an SEM. The deflection system moves the probe over the specimen surface along a line and then displaces the probe to a position on the next line for scanning, so that a rectangular raster is generated on the specimen surface. The signal electrons emitted from the specimen are collected by a detector, amplified, and used to reconstruct an image, according to one-to-one correlation between scanning points on the specimen and picture points on a screen of a cathode ray tube (CRT) or liquid crystal display. The deflection system of the electron probe is controlled by two pairs of electromagnetic coils (scan coils). The first pair of coils bends the beam off the optical axis of the microscope. The second pair of coils bends the beam back onto the axis at the

pivot point of a scan. The apertures in an SEM, as shown in Figure 3.4, are mainly used for limiting the divergence of the electron beam in its optical path. The magnification of an SEM is determined by the ratio of the linear size of the display screen to the linear size of the specimen area being scanned. The size of the scanned rectangular area (raster) can be varied over a tremendously wide range. Thus, an SEM is able to provide image magnification from about 20X to greater than 100,000X. For low magnification imaging, an SEM is often more favorable than a light microscope (LM) because of the large depth of field in SEM. [10] In order to prepare the specimen for SEM/EDS analysis, the samples should be dried and fixed on a conductive tape to avoid charging of the particles due to interaction with high energy beam.

Figure 3.5 is an example of sample surface using the Back Scatter Detector (BSD). BSD is used as the samples such as ash which have elastic scattering of electrons which makes it difficult for secondary electron (SE) detectors to have proper images and scans. This can be avoided using BSD which are solid-state devices, often with separate components for simultaneous collection of back-scattered electrons in different directions. Detectors above the sample collect electrons scattered as a function of sample composition, whereas detectors placed to the side collect electrons scattered as a function of surface topography, these are usually SE detectors. This was the primary approach for all ash samples.

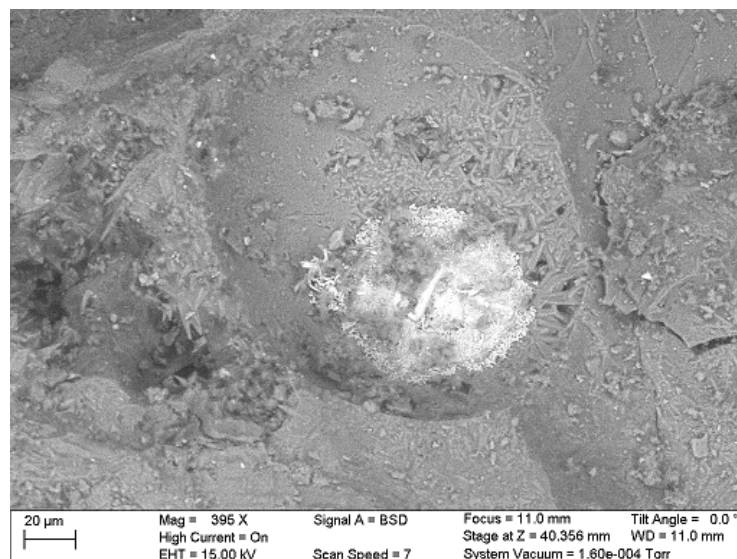


Figure 3.5: Example SEM image using Back Scatter Detector (BSD)

The EDS type of X-ray spectrometer is commonly included as a part of SEMs. The reason for using EDS is simply its compactness. With EDS in an electron microscope, we can obtain elemental analysis while examining the micro-structure of materials. EDS in an electron microscope uses a high energy electron beam (the same beam for image formation) as a source to excite characteristic X-rays from the specimen which is used by the X-ray spectrometer in the microscopes to identify the elements. EDS in an electron microscope is suitable for analyzing the chemical elements in microscopic volume in the specimen because the electron probe can be focused on a very small area. Thus, the technique is often referred to as microanalysis. The structure of EDS in an electron microscope is illustrated as in Figure 3.6, using an SEM system as an example. EDS

in the SEM is fundamentally similar to a stand-alone EDS except for the primary beam source. In the SEM, the electron beam aligns with the vertical axis of the microscope so that the Si(Li) detector has to be placed at a certain angle from vertical. The angle between the surface plane of the specimen and detector is called the take-off angle and is often referred to as the angular position of the detector. The take-off angle can be changed by rotating the specimen surface with respect to the detector. For a low take-off angle, a rough surface may interfere with collection of X-ray photons emitted from a valley area. Such problems do not occur if the specimen has a microscopically flat surface. [10]

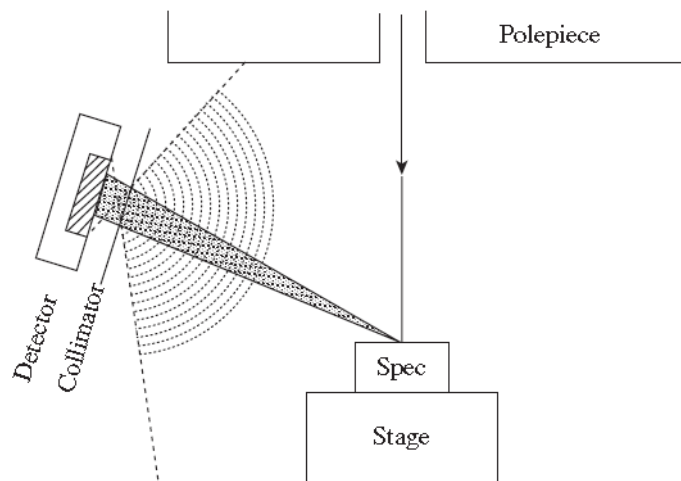


Figure 3.6: EDS schematic

### 3.2.4 Inductively coupled plasma atomic emission spectroscopy

ICP-AES (Inductively coupled plasma atomic emission spectroscopy), is a type of emission spectroscopy that uses the inductively coupled plasma to produce excited atoms and ions that emit electromagnetic radiation at wavelengths characteristic of a particular element. It is a flame technique with a flame temperature in a range from 6000 to 10000 Kelvin. It is also a solution technique & standard silicate dissolution methods are employed. The intensity of this emission is indicative of the concentration of the element within the sample. An intense electromagnetic field is created within the coil by the high power radio frequency signal flowing in the coil. This RF signal is created by the RF generator which is, effectively, a high power radio transmitter driving the "work coil" the same way a typical radio transmitter drives a transmitting antenna. Typical instruments run at either 27 or 40 MHz. The argon gas flowing through the torch is ignited with a Tesla unit that creates a brief discharge arc through the argon flow to initiate the ionization process. Once the plasma is "ignited", the Tesla unit is turned off. The argon gas is ionized in the intense electromagnetic field and flows in a particular rotationally symmetrical pattern towards the magnetic field of the RF coil.

A stable, high temperature plasma of about 7000 K is then generated as the result of the inelastic collisions created between the neutral argon atoms and the charged particles. A peristaltic pump delivers an aqueous or organic sample into an analytical nebulizer

where it is changed into mist and introduced directly inside the plasma flame. The sample immediately collides with the electrons and charged ions in the plasma and is itself broken down into charged ions. The various molecules break up into their respective atoms which then lose electrons and recombine repeatedly in the plasma, giving off radiation at the characteristic wavelengths of the elements involved. Within the optical chamber, after the light is separated into its different wavelengths (colours), the light intensity is measured with a photomultiplier tube or tubes physically positioned to "view" the specific wavelength(s) for each element line involved, or, in more modern units, the separated colors fall upon an array of semiconductor photodetectors such as charge coupled devices (CCDs). In units using these detector arrays, the intensities of all wavelengths (within the system's range) can be measured simultaneously, allowing the instrument to analyze for every element to which the unit is sensitive all at once. Thus, samples can be analyzed very quickly. The intensity of each line is then compared to previously measured intensities of known concentrations of the elements, and their concentrations are then computed by interpolation along the calibration lines. [11]. The sample preparation protocol is a modified EPA [9] "Method 1311". The method was modified to suite the objectives of the study. The Nitric acid content was increased by a factor of 5. This was done to obtain maximum dissolution. The 2 gram of sample was digested in a microwave heater with nitric acid for 8 hours at 120 degree celcius. Then the leachate was filtered and diluted before analyzing it with ICP-AES.

# Chapter 4

## Results and Discussion

There are three factors which can help understand the leaching behavior of ash.

- The matrix composition of the particle: The matrix of the ash can indicate the differences between an ash which leaches less and which does not. The type of particle matrix or the composition plays a huge role in acid attack resistance. A vitrified particle are more resistive towards an acid attack compared to an unvitrified particles.
- The type of the compounds formed by heavy metals after the thermal conversion process. As different compounds of same element have varying reactivity with acids.
- The elements released during the acid attacks can help in identifying the more stable ash particles as higher the leach lower the matrix stability.

These parameters can help in identification of the stability of the ash as compound structure and compound itself play an important role in reactions. The three factors can be translated as reactivity of chemical species present in ash and accessibility of these reactive species to the attacking chemicals such as acids. Therefore, helping in understanding the leaching behavior ash and facilitating in formulating a method to restrict leaching and finding a suitable maker element or a property of ash.

### 4.1 Matrix of the ash particle

Microanalysis of ash particles showed that the micro-structure and composition varied among the ash particles. The large particles (size greater than 3/8 inch) had numerous sites with elemental metal deposits on its surface. In addition to these sites the surface of particles were found to be less porous and similar to a vitrified particle. Figures 4.1 and 4.2 are an example of how the vitrified surfaces look in an SEM image compared to unvitrified ash particles from different sources. Figure 4.1a and 4.2a are both the SEM images of large particles and they are from different sources (*4.1a 4.1b from source G and 4.2a 4.2b from source D*), when compared to 4.1b and 4.2b, it can be observed that the surface morphology and mirco-structure are very much unlike. 4.1a and 4.2a have a smother surface which is an indication of compact and glassy surface or vitrified surface. They also have localized elemental metal deposits which can identified as the bright spots in the image which were absent in smaller particles(4.1b and 4.2b).

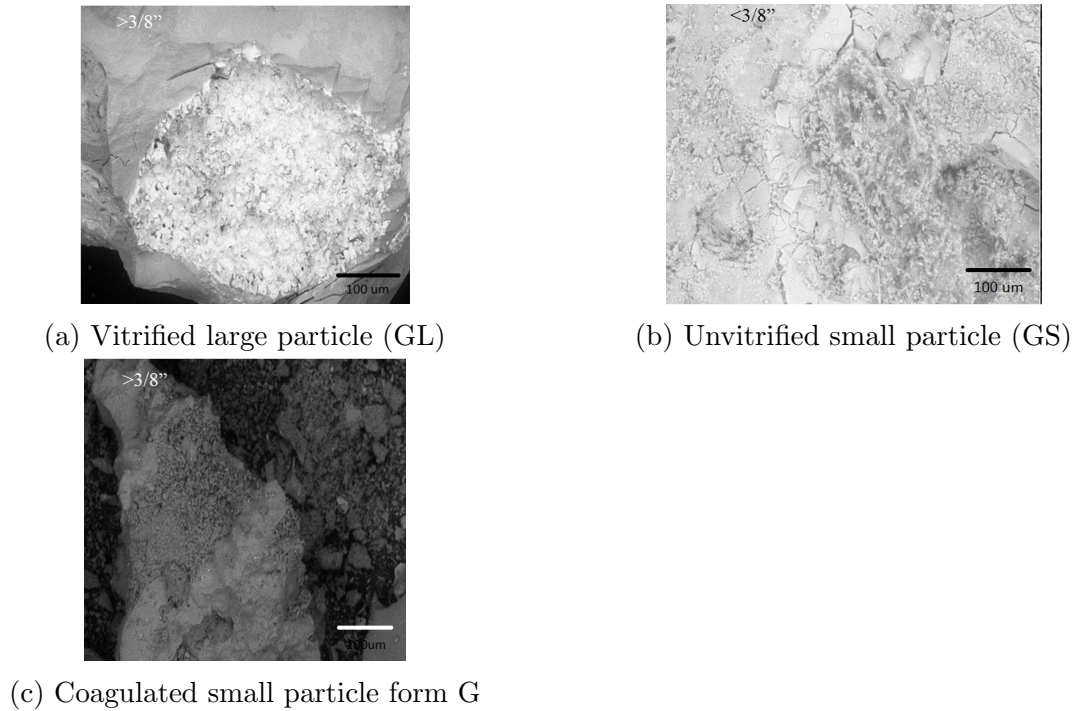


Figure 4.1: Comparison of large (GL) and small particles (GS) from source G

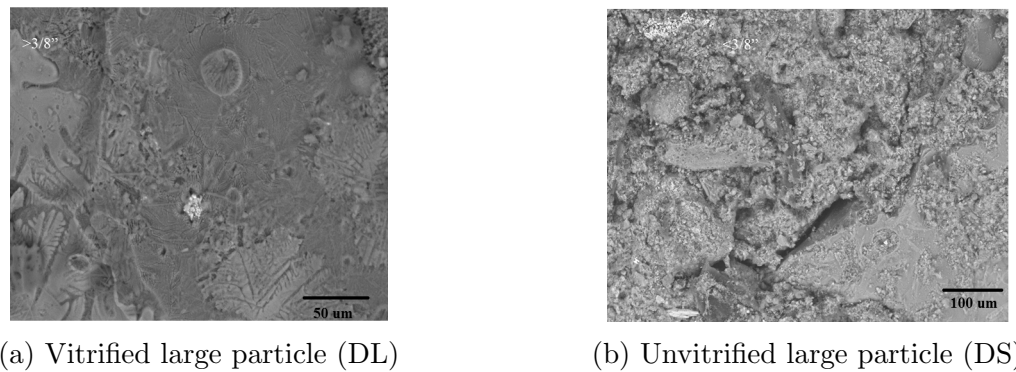


Figure 4.2: Comparison of large (DL) and small particles (DS) from source D

However, there were some large particles which did not exhibit the characteristics mentioned above for the large particles. But, a further analysis of these samples showed that these were in fact coagulated small particles forming larger false particle (Figure 4.1c). These larger false particles have low mechanical strength and start to crumble at small pressures (crumbles when pinched). The large particles collected after the sieve separation consisted of about 30% such coagulated particles. These coagulated large particles exhibited the same elemental composition as the small particles. This concludes that the smaller particles were formed after deformation of the larger particles under normal operating stresses during the transportation and collection of the ash. The extent of vitrification of ash and the process plays a huge role in formation of these smaller particles from large ones. If the ash is partially vitrified, then the particle tend to break in smaller parts which might be less  $3/8''$  inch. Ash produced during the thermal conversion process do not operate at high temperatures constantly, it might be possible that some particles get vitrified on outer surface of the particle. Ash also goes through a quenching

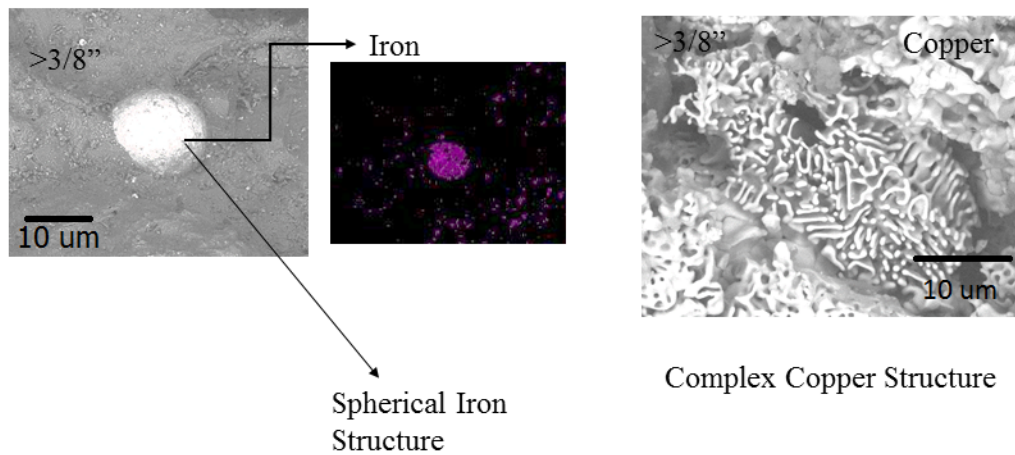
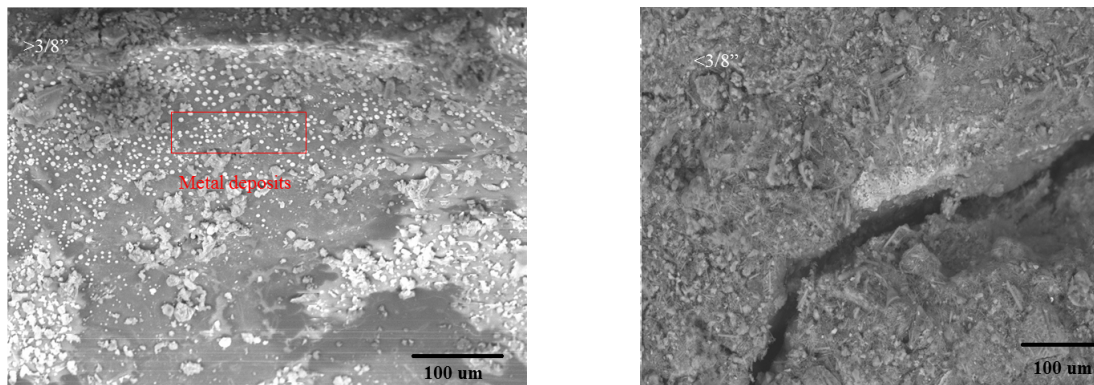


Figure 4.3: Iron and copper deposit on large ash particle surface

process which can also attribute to formation brittle surfaces or particles for some ash. These particles then mechanical stress of transportation can deform or break to make smaller particles.



(a) Metal spheres on large ash particle surface (b) Film metal deposition on smaller particles

Figure 4.4: Comparison of different types of depositions on ash particle surface

Although, there was an absence of concentrated metal deposits as shown in Figure 4.3 on the smaller particles. These elemental deposits can be found on all the large particles from different sources. These deposits on the surface was verified with EDS (elemental analysis) coupled with elemental mapping of the surface. Figure 4.3 is an example result. The center image is the map of iron on the surface image present on the left. The entire bright area on the image is an iron deposit without any other contaminations. This specific phenomenon was not to be found on smaller particles. However, some smaller ash particles showed a metal film deposition(Figure 4.4b) on its surface which was unlike the globule or structured metal deposits on the larger particles(Figure 4.4a) marked by the box. The metal film deposit present in Figure 4.4b is the slightly bright patch at the center of Figure 4.4b image.



Other major differences lies between composition of large and small particles. The percentage of major elements present in the large and small particles vary. Table 4.1 shows the elements present in ash on weight basis. It can inferred from the table that large particles will have higher silicon content compared to the smaller counterparts. This is a very crucial observation as this indicates presence of silicate compounds. Further, when ever both large and small particles have high silicon content the ash from that source shows a good TCLP behavior such as the ash from source F (FL and FS). The sample from source F showed small leaching of lead and also had high calcium and silicon presence. The TCLP data reported in this document was carried out on unsegregated ash sample, so the data consistent with industrial standards. The TCLP method, EPA (Environmental protection Agency) Method 1311 was a followed for this data set. The threshold limit is 5 mg/kg. [9]. Presence of high silicon in ash and simultaneously good behavior of ash concludes that presence of a silicate compound is necessary to restrict the leaching. Now the question arises how does silicon participate in this behavior of ash?.

Sample ID	TCLP Pb data (mg/kg)	Iron (w/w %)	Aluminum (w/w %)	Calcium (w/w %)	Silicon (w/w %)
AL	0.132/3.62	8.93	3.01	20.87	14.18
AS		1.1	3	29.87	3.08
BL	1.57	48.02	3.48	16.02	8.97
BS		1.05	3.96	20.62	1.98
CL	4.61	3	4.5	23	13.6
CS		4.24	3.18	40.2	2.3
DL	1.57	2.85	4.69	20.72	13.25
DS		0.4	3.9	22.6	1.8
EL	4.61	39.8	2.38	7.51	11.37
ES		2.13	2.15	29.1	4.82
FL	0.311	5.45	4.16	23.4	13.0
FS		-	4.88	14.72	21.44
GH	3.928	35.1	2.78	5.83	6.75
GL		3.26	8.34	20.36	6.54
GS		12.35	7.91	20.45	6.25

Table 4.1: SEM / EDS Measurement of Composition (% w/w)

The answer could be partially found in EDS mapping of the ash particle surface. Figure 4.5 is a perfect example of encapsulation by vitrification. Figure 4.5a is the electron image of a site on a vitrified particle, the adjacent Figure 4.5b shows the mapping of iron in red on the surface which is surrounded by aluminum (blue). Similar maps for iron (red) and silicon (yellow) and calcium (green) are show in Figures 4.5c and 4.5d, respectively. This concludes that the iron is encapsulated in calcium aluminum and silicon matrix. Thus suggesting the surrounding made of calcium aluminum silicon compound. This was then confirmed by XRD as it showed a compound gehlenite ( $\text{Ca}_2\text{Al}_2\text{SiO}_7$ ). So, the vitrified ash has a resilient (resistive to acid attacks) matrix made of Calcium, Aluminum and Silicon.



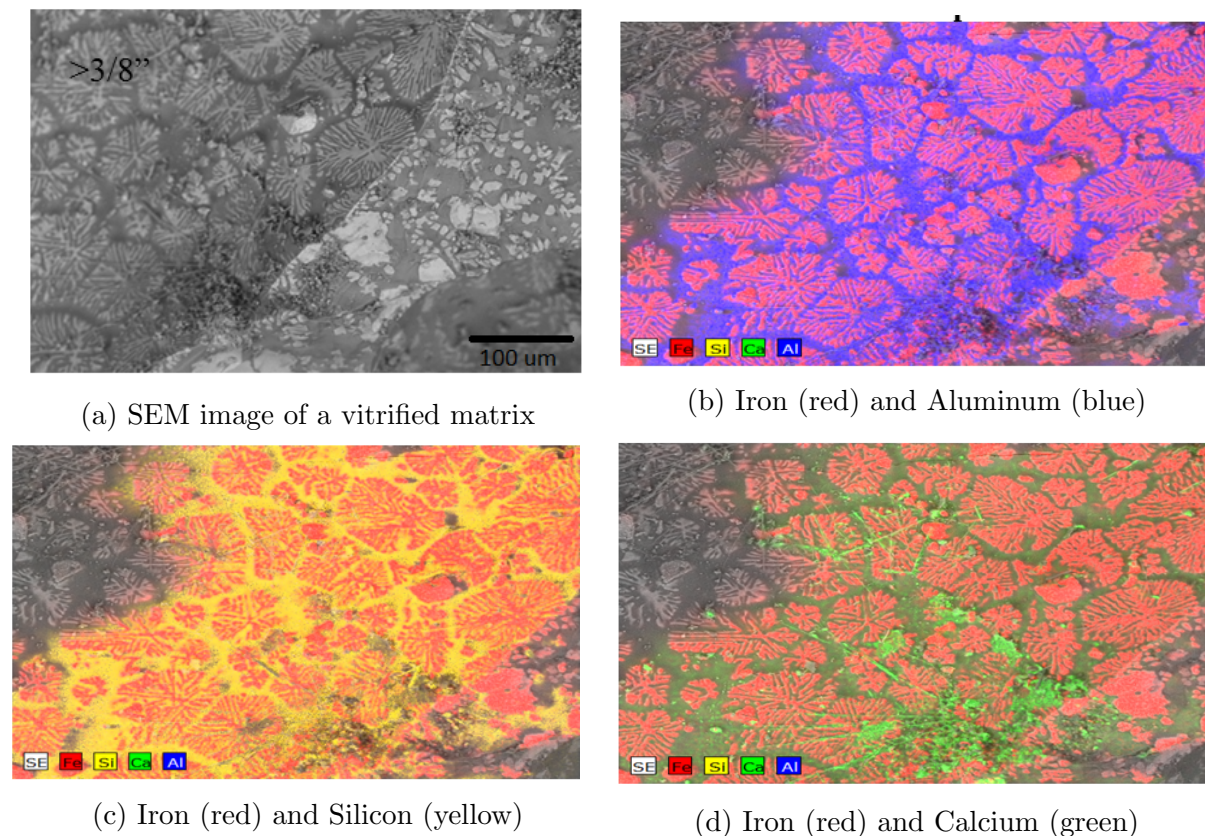


Figure 4.5: Cluster of Iron rich particles trapped in a vitrified ash majorly made of Aluminum, Silicon and Calcium. (a) SEM image of a vitrified matrix; b), c) and d) show iron (red), aluminum(blue), silicon (yellow)and calcium (green)

## 4.2 Variation in compounds

X-ray diffraction spectroscopy was primarily used to identified the crystalline compounds present in the ash. Common compounds present in ash are calcium carbonate ( $\text{CaCO}_3$ ), silicon dioxide ( $\text{SiO}_2$ )and Iron oxide ( $\text{Fe}_2\text{O}_3$ ). These two compounds dominate the crystalline composition of the ash. The large particles showed an additionally compound know as gehlenite ( $\text{Ca}_2\text{Al}_2\text{SiO}_7$ ). Which as described earlier is the compound associated with the vitrified particle.  $\text{Ca}_2\text{Al}_2\text{SiO}_7$  is the vitrified compound species which forms matrix to encapsulate metals and restrict metals to the attacking chemicals such as acids. Lead oxides present in the ash were also identified and ash from different sources showed various types of lead compounds. Table 4.2 shows the lead compound identified, it is clear that compound type can be directly correlated to TCLP data. The ash samples having  $\text{PbO}$  had higher TCLP number which points out towards the unstable behavior of the ash. Ash with  $\text{PbO}_2$  present showed very good leaching behavior. The lead compounds resistance to disassociation during an acid attack varies and the order is given below.

Stability of lead compounds under acid attack in decreasing order



Sample ID	Lead compound type	TCLP Pb data (mg/Kg)
AL	$\text{Pb}_3\text{O}_4$	0.132/3.62
AS		
BL	$\text{PbO}$	1.57
BS		
CL	Lead silicate	4.61
CS		
DL	-	1.57
DS		
EL	$\text{PbO}$	4.61
ES		
FL	$\text{PbO}_2$	0.311
FS		
GH	$\text{PbO}$	3.928
GL		
GS		

Table 4.2: Compound type of lead from XRD DATA (Regulatory threshold is 5ppm)

Figure 4.6 is an example of XRD scans of the ash from two different source. It can seen from the XRD graph in Figure 4.6 that lead has different oxidation state in the ash from two sources. Thus forming Lithrage ( $\text{PbO}_2$ ) in ash from source G and Lead oxide ( $\text{PbO}_2$ ) in from source ash F.

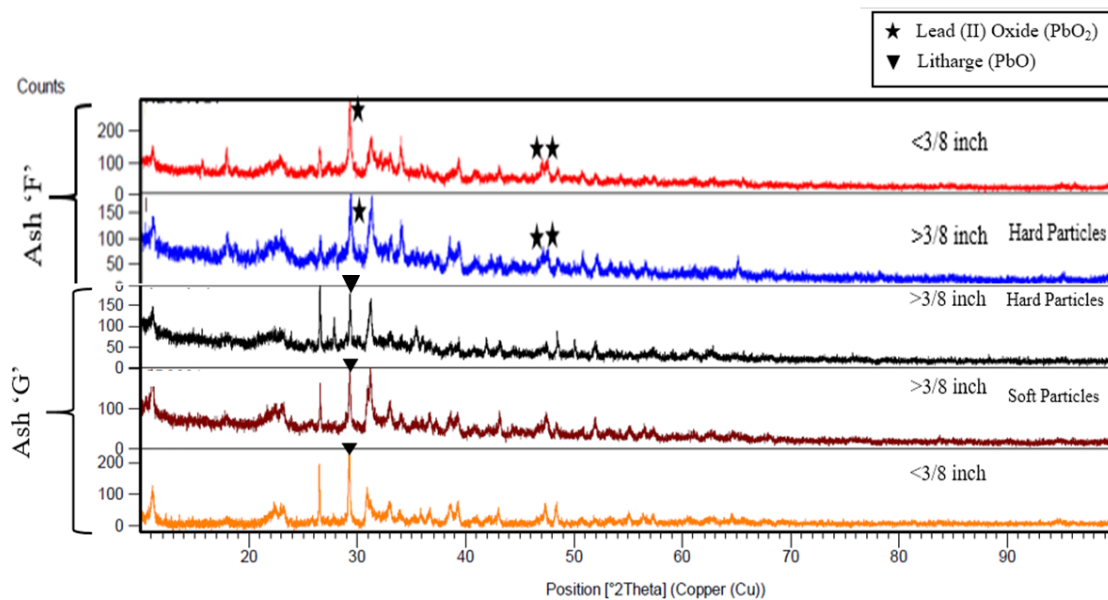


Figure 4.6: Comparison of XRD of Ash from source F &amp; G for Lead compounds

Lithrage ( $\text{PbO}$ ), are normally formed at higher temperatures compared to Lead oxide ( $\text{PbO}_2$ ). The difference in temperatures is about  $250^\circ\text{C}$ . This variation in oxidation state of the Pb caused by varying operating temperature is one of the main factors responsible for the extreme leaching behavior. The initial predications based on the literature and

XRD data concluded that the operating temperature for facility G was higher than F. When operating temperature for source G facility was compared to F, it was in compliance with the laboratory predictions and the facility G was operating at a higher temperature. Since, the source G operates at a higher temperature than F, the lead oxide is converted to litharge. This becoming the second factor influencing the leaching behavior in addition to matrix variations.

### 4.3 Leaching and behavior under acid attack

The leaching test or the ICP-OES test provided a number of insights into the stability of the matrix of ash. As mention earlier in chapter 3, ICP test are performed by digesting the solids in an acidic solution to disassociate the compounds which are ultimately detected and reported. As ash is a by product of high temperature combustion , it is impossible to completely disassociate the ash into the acidic solution even with stronger acids such as hydrofluoric acid. The maximum disassociation is averaged about 40% by weight, although this is very low for major elements. Thus only trace metals such as lead, arsenic, copper etc. which are assumed to be disassociated into the solution and are representative of the sample set. This test served two purposes, to quantify trace amounts of lead and to use iron and aluminum as markers to quantify the performance of ash under an acidic attack.

Sample ID	TCLP Pb data (mg/Kg)	Lead(ppm)	Iron(ppm)	Aluminum(ppm)	Al/Fe
AL	0.132/3.6	192.6	14401.2	9535.9	0.6
AS		338.9	6685.9	12990.2	1.9
BL	1.5	154.6	32301.2	14560.5	0.4
BS		1468.6	11203.6	33840.2	3.0
CL	4.6	294.3	18894.9	24460.8	1.2
CS		1122.9	16269.3	30287.2	1.8
DL	1.57	432.5	14092.6	35867.6	2.5
DS		135.8	9064.9	21284.6	2.3
EL	4.6	385.2	20954.7	12183.1	0.5
ES		327.9	11315.0	22692.4	2.0
FL	0.3	262.1	1643.4	11498.5	6.9
FS		171.0	1186.4	10168.4	8.5
GH	3.9	483.8	25343.1	12699.0	0.5
GL		251.2	43381.2	10098.9	0.2
GS		428.2	10132.8	15761.6	1.5

Table 4.3: ICP-OES Concentrations in Leachate, HNO<sub>3</sub> acid attack

Table 4.3 shows the concentration of lead iron and aluminum (ppm) in the leachate against TCLP and aluminum to iron ratio. The concentration of three elements is always high in smaller particles except for in FL and FS. The higher concentration of iron and aluminum indicate easier disassociation of the ash particles. This indicates a weaker ash matrix when compared to large particles. Large particles mostly constitute vitrified

particles which have a stronger silicate matrix. Thus making larger particles more resilient towards acid attack and releasing lesser iron and aluminum. Additionally, the EDS analysis indicates that the aluminum concentration (Table 4.1) values in large and small are very close. This makes perfect marker for testing the matrix stability under acid attack. Likewise, the iron concentration (Table 4.1) for certain large particles can be compared to give more comprehensive idea of the matrix stability.

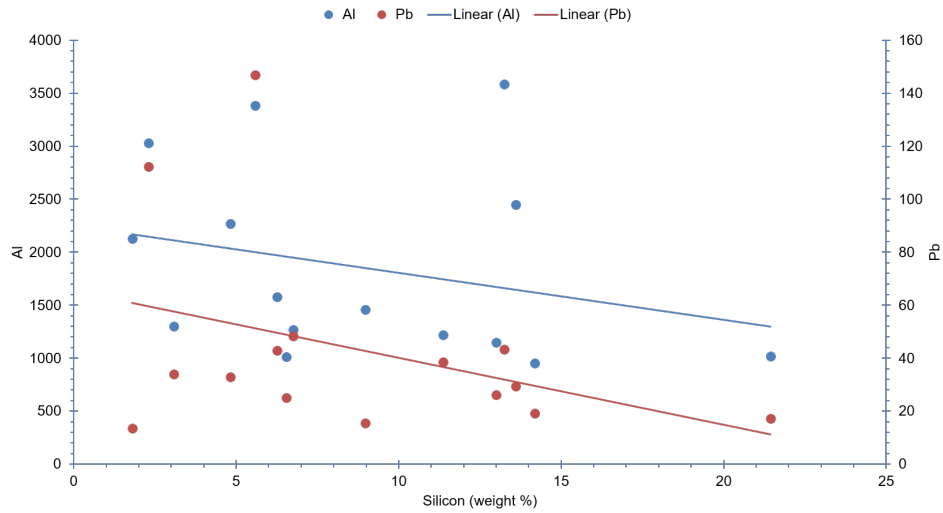


Figure 4.7: Silicon vs Lead/ Aluminum (ppm)

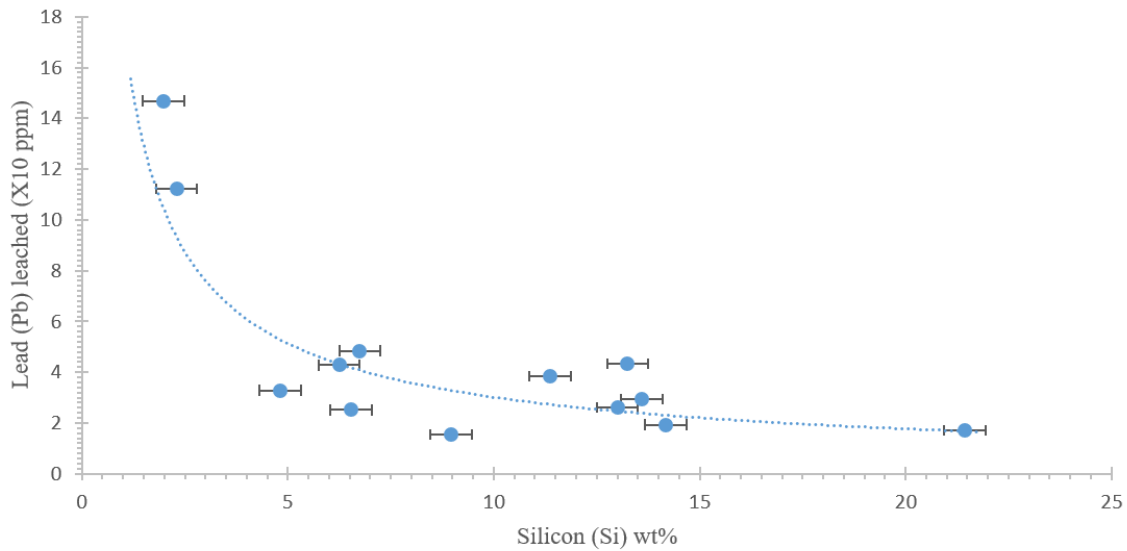


Figure 4.8: Silicon vs Lead leached

These two elements can be then correlated with silicon weight % present in ash. Figure 4.7 attempts to show the correlation between Silicon, Aluminum and Lead. The left y-axis of the graph is aluminum concentration and right y-axis is Lead concentration plotted against silicon percentage (weight%). With the increase in silicon the leaching of iron and aluminum decreases. It can be seen these concentrations do not give a clear trend or correlation as the variability in the ash composition effects the concentration in each

sample. However, this gives a general direction to look for a suitable indicator for leaching behavior. The only valuable information that can be inferred is that silicon and leaching of lead is correlated. This is further supported when we look at lead leached and silicon weight percentage in Figure 4.8. The y-axis in Figure 4.8 is the amount of lead leached and the x-axis is the silicon weight %. The amount of lead leached can be correlated to silicon present in the ash by a power curve and by the equation  $y = 17.69 * x^{(-0.769)}$ . This dependency on silicon is based on the matrix of the ash particles, as it was illustrated earlier using SEM and mapping analysis that some ash particles have matrix made up of calcium-aluminum-silicates (CAS). These CAS matrices encapsulate most of metals including lead. Thus, restricting acid attack and in effect reducing the amount of lead leached. This can be also observed in Figure 4.9, it is a plot of aluminum released during an acid attack (aqua-regia) with silicon content on the x-axis. Except for two anomalies most of the data set follow a similar profile. This in lieu of earlier findings strengthens the assumption that a vitrified silicon rich particle is highly resilient towards acid attacks and has good stable TCLP behavior. This phenomenon is mostly due to presence of CAS, which helps in improving the leaching properties of the ash. It can also be determined as to what is the upper-lower limit of the silicon for which there is no significant performance change using the equation for the Pb-Si dependence. Table 4.4 presents hypothetical leached values for a given silicon in ash particles using the equation  $y = 17.69 * x^{(-0.769)}$ . Therefore, the upper-lower limit for silicon is 6 (upper) and 20 (lower) weight %. Beyond 20 wt.% the increase on Pb leach performance is marginal, it is 3% for every 1% increase in silicon.

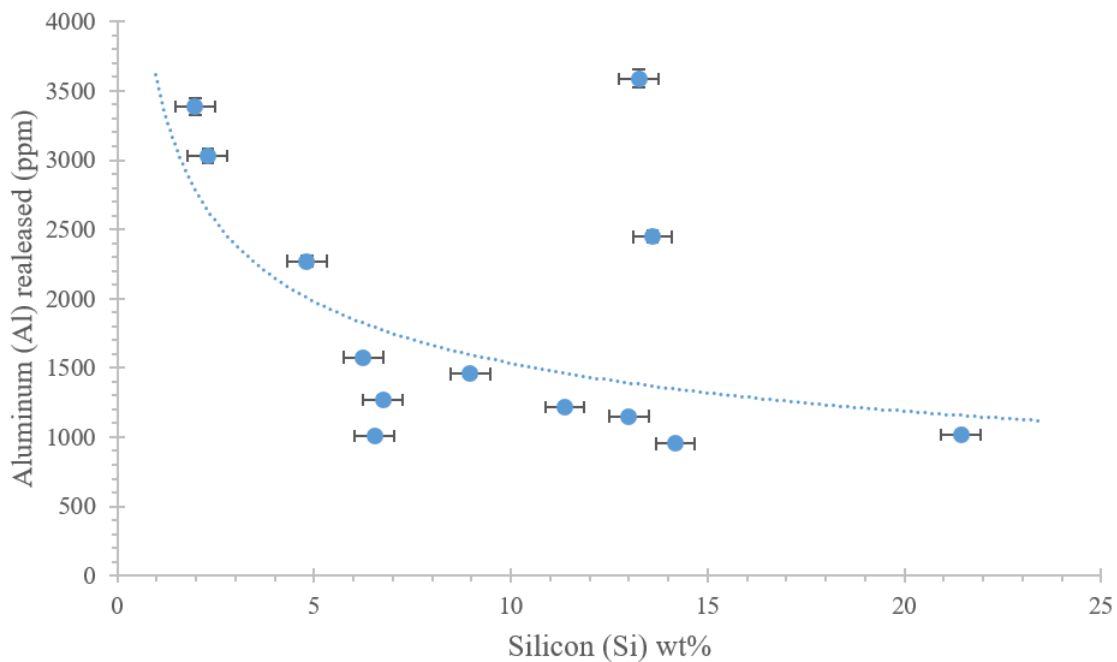


Figure 4.9: Silicon vs Aluminum released (during the acid attack)

Silicon (wt. %)	Lead Leached (calculated) (X10 ppm)
2	10.45
4	6.17
6	4.53
8	3.64
10	3.07
12	2.68
14	2.38
16	2.15
18	1.97
20	1.82
22	1.69
24	1.58
26	1.49
28	1.41
30	1.33
32	1.27
34	1.21
36	1.16
38	1.11
40	1.07
42	1.03
44	1
46	0.96

Table 4.4: Lead Leached (Calculated)

Considering the aluminum release trends it can be concluded that the Al is a good maker for the stability of the ash particles with respect to acid attacks. Additionally, the amount of silicon present in the ash can also be indicative of a good stable ash. As more silicon present can help in forming silicates other than quartz which will improve the leaching characteristics. These two elements can be considered as makers for ash stability. However, to test for stability will require an acid attack test similar to TCLP test which is not convenient in terms of industrial application as it has a longer turn around time for results. Using silicon as a maker will get results in a shorter time frame as it is straight SEM/EDS characterization which is faster.

## 4.4 Summary

Investigations concluded that the different oxidation states of element (Pb) and stability of ash matrix was the cause of the fluctuating leaching behavior in bottom ash from different facilities. Additionally, vitrification/sintering of ash by forming a Ca, Al and Si matrix can be an effective method of restricting availability of leachable compounds. The quantity of Aluminum and Silicon present in ash can be used as a marker

to identify/predict the leaching behavior. Additionally the three factors which can help understand and predict the leaching behavior of ash are:

1. **The matrix of ash particle:** The stronger the matrix the more resilient ash is towards an acid attack. From the above mentioned series of test it can be concluded that the vitrified silicon rich particles make a resilient matrix.
2. **Type of compound formed:** The toxic elements such as lead, arsenic etc. can achieve different oxidizing states depending on the operating temperatures. This can then result in formation of either a stable compound or an unstable compound. This parameter greatly effects the leaching behavior of the ash.
3. **Elemental Composition:** Aluminum release during an accelerated acid attack can be called a indicative phenomenon rather than a factor which effects the leaching behavior. The high release of Al indicates weak matrix and thus reiterating the first point. Silicon percentages in ash directly relate towards the leaching performance of the ash from waste thermal conversion plants. If the silicon by weight percent in ash is in the range of 6-20% it will perform better in TCLP test and have much stable matrix compared to ash with Si less than 6%.

Understanding these factors gives an insight and in future will allow us to control the leachate content. Thus making WtEs a more reliable and more safe option to divert the MSW from landfills and recycling facilities. One of the major findings that is presence of silicates in low leached particles can be implemented by simply adding more glass cullets in to the combustion process to increase the amount of vitrified ash and make the residue from WtE facilities less leach able and more usable. The other effect of adding silicates to the process would be formation of aluminum silicates which are a type of cementitious material which can be used with construction materials. Therefore, providing an alternate route for ash than to sending it to landfills. This will help in closing the material cycle and making waste disposal a more sustainable effort.

Sample ID	Silicon% (EDS)	Mechanical strength	Elemental Iron on particles (EDS)	Lead (ppm) (ICP)	Aluminum (ppm) (ICP)	Lead compound type	TCLP Pb data (mg/Kg)
AL	14.18	Hard to crush	Yes	192.6	9535.964	Pb3O4	0.132/3.62
AS	3.08	Easily crushed	No	338.9	12990.21		
BL	8.97	Hard to crush	Yes	154.6	14560.52	PbO	1.57
BS	1.98	Easily crushed	No	1468.6	33840.22		
CL	13.6	Hard to crush	Yes	294.3	24460.8	Lead silicate	<b>4.61</b>
CS	2.3	Easily crushed	No	1122.9	30287.22		
DL	13.25	Hard to crush	Yes	432.5	35867.63	-	1.57
DS	1.8	Hard to crush	No	135.8	21284.62		
EL	11.37	Hard to crush	Yes	385.2	12183.18	PbO	<b>4.61</b>
ES	4.82	Hard to crush	No	327.9	22692.45		
FL	13.0	Easily crushed	No	262.1	11498.5	PbO2	<u><b>0.311</b></u>
FS	21.44	Easily crushed	No	171.0	10168.41		
GH	6.75	Easily crushed	Yes	483.8	12699.04	PbO	<b>3.928</b>
GL	6.54	Hard to crush	Yes	251.2	10098.97		
GS	6.25	Easily crushed	No	428.2	15761.69		

Table 4.5: Summary



# References

- [1] D. Shin, *Genration and disposition of municipal Solid Waste(MSW) in United States - A National Survey*. PhD thesis, Columbia University Earth Engineering Center, New York City, 2014.
- [2] L. Rigamonti, A. Falbo, and M. Grosso, “Improving integrated waste management at the regional level: the case of lombardia,” *Waste Management & Research*, p. 0734242X13493957, 2013.
- [3] P. Bajpai, *Recycling and deinking of recovered paper*. Elsevier, 2013.
- [4] E. Nolley, J. Barlow, and D. Paul, “Mechanical properties of polypropylene-low density polyethylene blends,” *Polymer Engineering & Science*, vol. 20, no. 5, pp. 364–369, 1980.
- [5] A.-H. I. Mourad, “Thermo-mechanical characteristics of thermally aged polyethylene/polypropylene blends,” *Materials & Design*, vol. 31, no. 2, pp. 918–929, 2010.
- [6] R. Strapasson, S. Amico, M. Pereira, and T. Sydenstricker, “Tensile and impact behavior of polypropylene/low density polyethylene blends,” *Polymer testing*, vol. 24, no. 4, pp. 468–473, 2005.
- [7] M. Castro, J. Remmerswaal, M. Reuter, and U. Boin, “A thermodynamic approach to the compatibility of materials combinations for recycling,” *Resources, Conservation and Recycling*, vol. 43, no. 1, pp. 1–19, 2004.
- [8] T. Rosenqvist, *Principles of extractive metallurgy*. Tapir academic press, 2004.
- [9] E. P. Agency, *Method 1311*.
- [10] Y. Leng, *Materials characterization: introduction to microscopic and spectroscopic methods*. John Wiley & Sons, 2009.
- [11] S. J. Hill, *Inductively coupled plasma spectrometry and its applications*, vol. 8. John Wiley & Sons, 2008.
- [12] A. forest and P. r. Paper Association, *American forest and Paper Association, Paper recycles*. [Online], 2014.
- [13] Z. W. I. Alliance, *Zero Waste definition*. [Online], Mar. 2013.
- [14] F. D. of environmental Protection, *Annual Report 2012*. [Online], 2012.

- [15] M. R. Gent, M. Menendez, J. Torano, and S. Torno, “Optimization of recovery of plastics for recycling by density media separation,” *Resources, Conservation and Recycling*, vol. 55, pp. 472–482, 2011.
- [16] B. Gershman and Bratton, *Waste characterization*. 2014.
- [17] J. Hopewell, R. Dvorak, and E. Kosior, “Plastics recycling: challenges and opportunities,” *Philosophical transactions of Royal Society B*, no. 364, pp. 2115–2126, 2009.
- [18] R. C. Howard, “The effects of recycling on paper quality,” *Journal of Pulp and Paper Science*, vol. 16, no. 5, p. J143, 1990.
- [19] A. Lopez, I. de Marco, B. M. Carballero, M. Laresgoiti, and A. Adrados, “Pyrolysis of Municipal Plastics wastes: Influences of raw material composition,” *Waste Management*, vol. 30, pp. 620–627, 2010.
- [20] H. Shaikh and J. Luo, “Identification, validation and application of a cellulose specifically to improve the runnability of recycled furnishes,” in *Proceedings of the ninth international technical conference on pulp, paper and allied industry (Paperex’09)*, New Delhi, India, 2009.
- [21] N. J. Themelis and L. Arsova, *Identification and assessment of available technologies for materials and energy recovery from flexible packaging waste (FPW)*. Columbia University Earth Engineering center, New York City, 2010.